

Multiple Time Scales of Temporal Response in Pyramidal and Fast Spiking Cortical Neurons

Giancarlo La Camera,* Alexander Rauch,* David Thurbon, Hans-R. Lüscher, Walter Senn, and Stefano Fusi

Institute of Physiology, University of Bern, Bülhplatz 5, Switzerland

Submitted 30 April 2006; accepted in final form 16 June 2006

La Camera, Giancarlo, Alexander Rauch, David Thurbon, Hans-R. Lüscher, Walter Senn, and Stefano Fusi. Multiple time scales of temporal response in pyramidal and fast spiking cortical neurons. *J Neurophysiol* 96: 3448–3464, 2006. First published June 28, 2006; doi:10.1152/jn.00453.2006. Neural dynamic processes correlated over several time scales are found in vivo, in stimulus-evoked as well as spontaneous activity, and are thought to affect the way sensory stimulation is processed. Despite their potential computational consequences, a systematic description of the presence of multiple time scales in single cortical neurons is lacking. In this study, we injected fast spiking and pyramidal (PYR) neurons in vitro with long-lasting episodes of step-like and noisy, in-vivo-like current. Several processes shaped the time course of the instantaneous spike frequency, which could be reduced to a small number (1–4) of phenomenological mechanisms, either reducing (adapting) or increasing (facilitating) the neuron's firing rate over time. The different adaptation/facilitation processes cover a wide range of time scales, ranging from initial adaptation (<10 ms, PYR neurons only), to fast adaptation (<300 ms), early facilitation (0.5–1 s, PYR only), and slow (or late) adaptation (order of seconds). These processes are characterized by broad distributions of their magnitudes and time constants across cells, showing that multiple time scales are at play in cortical neurons, even in response to stationary stimuli and in the presence of input fluctuations. These processes might be part of a cascade of processes responsible for the power-law behavior of adaptation observed in several preparations, and may have far-reaching computational consequences that have been recently described.

INTRODUCTION

Neural dynamic processes correlated over several time scales have been found in a variety of preparations, including the cerebral cortex. Reported early in the peripheral nervous system of invertebrates (Thorson and Biederman-Thorson 1974 and references therein), these processes have been found more recently in cat auditory cortex neurons, where stimulus-specific adaptation accounts for the difference in responses to rare versus common stimuli over an extended range of time scales (a few hundred milliseconds to hundreds of seconds) (Ulanovsky et al. 2004). In cat auditory nerve fibers (Lowen and Teich 1996) and in the lateral geniculate nucleus (LGN) of the cat thalamus (Lowen et al. 2001), neural activity can exhibit long-range correlations spanning multiple time scales.

Having been collected in vivo, this experimental evidence raises the possibility that the interaction between neurons could underlie the expression of multiple time scales. However, the existence of ion channels with different kinetics suggests that

individual neurons may be equipped to produce dynamic activity which correlates on multiple time scales. For example, Spain et al. (1991) reported the existence of (at least) two transient potassium currents in the large pyramidal (PYR) neurons of the layer 5 of cat sensorimotor cortex. These currents decayed with different time scales (~20 ms vs. ~10 s) comparable to the time constants of the fastest and slowest adaptation processes previously found in PYR neurons by Rauch et al. (2003). However, no quantitative accounts of the number and the properties of those processes have been reported nor has a similar study been undertaken in neurons the firing patterns of which distinctively differ from the pyramidal or the sensory type, like e.g., fast spiking (FS) interneurons (McCormick et al. 1985).

We analyzed in detail the response of FS and PYR neurons in vitro to long-lasting, noisy stimuli with stationary statistics. The noisy stimuli are meant to imitate the synaptic currents that are observed in vivo in intracellular recordings (Destexhe et al. 2001; Paré et al. 1998). When the input currents were strong enough, the neural response was highly nonstationary for both FS and PYR neurons. The largest variations of the firing frequency over time were observed in the initial phase of the stimulation, but detectable nonstationarities could be seen in the late response of the stimulated cell. This is an indication that several mechanisms operating on multiple time scales determine the response of a neural cell to a stimulus with stationary statistics. We used a novel approach to characterize quantitatively the neuronal response. It consists of two steps: first, a simple model of an integrate-and-fire (IF) neuron was fitted to the late, quasi-stationary responses of the neurons to a variety of input currents (Rauch et al. 2003). Dynamic components were ignored because the variations of the firing rate, although still detectable, were small compared with the firing rates themselves. The second step is an extended model with time-varying processes (adaptation) that was fitted to the temporal response of the neurons from the same set of data, with the neuron parameters set by the previous fit. This second step gave the parameters of the time-varying processes (magnitude and time constant). Based on a detailed analysis performed on those parameters, we report quantitative evidence that multiple time scales are at play in both PYR and FS neurons. We also show that a simple spiking model can provide quite a detailed account of firing rate dynamics of cortical neurons probed in an in-vivo-like environment. Finally, we study the distribution of the functional parameters across cells.

* G. La Camera and A. Rauch contributed equally to this work.

Present address and address for reprint requests and other correspondence: G. La Camera, Laboratory of Neuropsychology, National Institute of Mental Health, National Institutes of Health, 49 Convent Dr, Bethesda, MD 20892-1148 (E-mail: lacamerag@mail.nih.gov).

The costs of publication of this article were defrayed in part by the payment of page charges. The article must therefore be hereby marked "advertisement" in accordance with 18 U.S.C. Section 1734 solely to indicate this fact.

Multiple time scales in cortical neurons might profoundly affect sensory processing and, more generally, neural computation, as proposed by recent theoretical studies (e.g., Brenner et al. 2000; Drew and Abbott 2006; Fairhall et al. 2001) that we briefly review in the Discussion.

METHODS

Experimental preparation and recordings

The experimental preparation was as described previously (Rauch et al. 2003). Briefly, 300 μm thick parasagittal slices of rat somatosensory cortex were prepared from 15- to 40-day-old female and male Wistar rats according to the institutional guidelines. The preparation was done in ice cold extracellular solution using a Campden vibratome (752M, Campden Instruments). Slices were incubated at 37° for 25 min and afterward left at room temperature until transferred to the recording chamber. The cells were visualized by infrared differential interference contrast videomicroscopy using a Newwicon camera (C2400, Hamamatsu City, Japan) and an infrared filter (RG9, Schott Mainz) mounted on an upright microscope (Axioscope FS, Zeiss).

We recorded in current-clamp whole cell configuration from the soma of layer 5 (L5) and layer 2/3 (L2/3) FS (McCormick et al. 1985) neurons and L5 PYR neurons. Recordings and stimulations were made with an Axoclamp-2A amplifier (Axon Instruments) in combination with Clampex 8 (Axon Instruments). The access resistance and the capacitance were compensated using the bridge balance and the capacitance neutralization after having established the whole cell configuration. The data were low-pass filtered at 2.5 kHz with sampling frequency twice the filter frequency. The temperature of the external solution was 31–33° C. Neurons were visually identified, most of them were filled with biocytin (10 mM) and then stained according to the ABC procedure (Hsu et al. 1981). A standard criterion for classification of cells as FS neurons was used (see, e.g., Descalzo et al. 2005): short duration of action potentials (<0.5 ms at half height), fast after-spike repolarization, absence of firing rate adaptation in the first milliseconds of the spike train, a steep frequency-current curve around rheobase (see Figs. 1 and 4).

Slices were continuously superfused with an artificial cerebrospinal fluid containing (in mM) 125 NaCl, 25 NaHCO₃, 2.5 KCl, 1.25 NaH₂PO₄, 2 CaCl₂, 1 MgCl₂, and 25 glucose, gassed with 95% O₂-5% CO₂. The pipette solution contained (in mM) 115 K-gluconate, 20 KCl, 10 HEPES, 4 Mg-ATP, 0.3 Na₂-GTP, and 10 Na₂-phosphocreatine, pH adjusted to 7.3 with KOH. The measured osmolarity was between 310 and 325 mosm.

Stimulation protocol and main observables

The stimuli were fluctuating in time around an average value but were stationary in the following sense: they were completely characterized by their means and SDs, which were held fixed throughout the stimulation interval. We chose stimuli with virtually no temporal correlation, i.e., resembling white noise. Specifically, the input current was generated as an Ornstein-Uhlenbeck stochastic process by iterating the following expression

$$I(t + \Delta t) = I(t) - \frac{I(t)}{\tau_I} \Delta t + \frac{m_I}{\tau_I} \Delta t + S_I \sqrt{\frac{2}{\tau_I}} \xi_I \sqrt{\Delta t} \quad (1)$$

where ξ_I is a unitary Gauss distributed random variable, updated at every time step. The process was generated and injected at a rate of 5 kHz ($\Delta t = 0.2$ ms) and the correlation length τ_I was 1 ms. The resulting current $I(t)$ has a stationary Gauss distribution with mean m_I and variance s_I^2 (Cox and Miller 1965). Such a noisy stimulus is meant to emulate the synaptic barrage targeting a cortical neuron in vivo due

to fast excitatory and inhibitory inputs (Rauch et al. 2003). In a few cells we used $\tau_I = 5$ ms with similar results.

The $\{m_I, s_I\}$ space was systematically explored as follows: data points were collected at fixed s_I (ranging from 0 to 200 pA), stepwise increasing m_I from a subthreshold value up to nonstationary frequencies. The data with $s_I = 0$ (step current) were used to determine the threshold mean current I_{th} (the rheobase current), and the whole procedure served to establish the whole space of suitable $\{m_I, s_I\}$ pairs for the neuron under study. The pool of suitable $\{m_I, s_I\}$ pairs was then discretized and explored in random order to prevent correlations between time and one of the two parameters m_I, s_I . This randomized protocol was used to characterize the response function of the neuron, i.e., its mean firing rate as a function of m_I and s_I (more details in the following text). For each pair $\{m_I, s_I\}$, stimulation lasted 4 s. Between recordings, the stimulus was switched off and the neuron let to rest for 50–60 s. Some of the recordings were longer (≤ 10 s) to check that the high spike frequencies found could be sustained for longer stimulations. The first part of the neuronal response (0.5 s) was discarded when estimating the mean spike frequency.

The mean spike frequency, f , was estimated as the ratio between the total number of action potentials N_{sp} and the stimulus duration T . The confidence intervals (68%) of the experimentally measured frequencies were approximately given by $\Delta = (\Delta f^+ + \Delta f^-)/2$ with (Rauch et al. 2003)

$$\Delta f^\pm = \frac{1}{T} \left| \frac{1}{2} \pm \sqrt{N_{sp} + \frac{1}{4}} \right| \quad (2)$$

This formula corresponds, roughly, to a Poisson model for spike emission, corrected at low output rates: for large output rates the errors tend to be symmetrical and distributed as in a Poisson model of the spike count ($\propto \sqrt{N_{sp}}$), the longer the observation interval T , the smaller the confidence intervals; second, if no action potentials are observed in $(0, T)$, then the “true” output rate falls within the interval $(0, 1/T)$ with ~68% confidence. A derivation of Eq. 2 is given in the APPENDIX.

Particular care was taken to ensure that the response of the cell was consistent throughout the whole recording session. The cells were classified as *consistent* if: less than half of the pairwise differences between repeated recordings were out of the error range given by Eq. 2; at a given m_I , responses to current with different s_I preserved the sign, i.e., if $f(m_I, s_I) > f(m_I, s_I')$ in one recording, then the same order relationship is observed in all of the repeats of the same recording [$f(m_I, s_I)$ is the mean firing rate in response to a current characterized by m_I and s_I]. Only consistent cells were further analyzed.

A neuron’s response function is the collection of quasi-stationary firing rates in response to a set of stimuli with different means and SDs. We defined a spike train as *quasi-stationary* if its firing rate was constant over the recording interval or, in the presence of adaptation, if its maximal decrease in firing rate per second, δf , was below a given threshold, chosen to be 1 Hz/s for PYR neurons and 5 Hz/s for FS neurons (see also following text). The amount of frequency reduction was quantified by the index $\delta f = (f_{init} - f_{final})/\delta T$, where $\delta T = t_{final} - t_{init}$, and f_{init}/f_{final} is the frequency in a temporal window 1 s wide, centered around t_{init}/t_{final} (for example, if $T = 4$ s was the total duration of the stimulus, $t_{init} = 1$ s, $t_{final} = 3.5$ s, $\delta T = 2.5$ s). Although firing rate changes could be detected when the slowest components of adaptation were analyzed, they did not affect significantly the quality of the model fits to the response functions (the model fits are described in the next subsections). This was also the criterion for choosing the aforementioned thresholds for δf . Pearson’s linear correlation and nonparametric Kendall’s tau were used to assess the correlation between parameter δf and output firing rate f (across all recordings of each single neuron).

The coefficient of variability (CV) of the interspike intervals (ISIs) was estimated as the ratio between the SD and the mean of the ISIs. An initial portion of the spike train of 0.5 s was removed to evaluate

the CV on a stationary or quasi-stationary spike train only. The interval was chosen to be significantly longer than the duration of the fastest adaptation process (see RESULTS for more details).

Model response function

A leaky IF (LIF) model neuron endowed with a phenomenological model of spike frequency adaptation (Ermentrout 1998; Fuhrmann et al. 2002; Rauch et al. 2003) was used to describe quantitatively the response of the neurons. The output rate of the LIF neuron in quasi-stationary conditions, f , is described accurately by the solution of the self-consistent equation (La Camera et al. 2004a; Rauch et al. 2003)

$$f = \Phi(m_I - \alpha f, s_I) \quad (3)$$

where $\{m_I, s_I\}$ are the average and the SD of the input current, α (pA · s) is a parameter quantifying adaptation, and Φ is the response function of the LIF model neuron, i.e.,

$$\Phi(m_I, s_I) = \left[\tau_r + \tau \int_{\frac{C V_r - m_I}{\sigma_I \sqrt{\tau}}}^{\frac{C \theta - m_I}{\sigma_I \sqrt{\tau}}} \sqrt{2} e^{x^2} (1 + \operatorname{erf}(x)) dx \right]^{-1} \quad (4)$$

where $\sigma_I = s_I / \sqrt{2\tau_r}$. The meaning of the parameters is as follows: C is the membrane capacitance, τ_r is the time constant of the input current (Eq. 1), τ_r is the absolute refractory period, θ is the threshold for spike emission, V_r is the reset potential after spike emission, τ is the membrane time constant, and $\operatorname{erf}(x) = (2/\sqrt{\pi}) \int_0^x dt e^{-t^2}$ is the error function.

Data analysis and fitting procedure

The theoretical $f(m_I, s_I)$ curves were fitted to the quasi-stationary data of consistent cells. The fit was achieved through a *Montecarlo* minimization (see e.g., Press et al. 1992) of the square difference between the measured (f_k^{exp}) and the model (f_k^{th}) firing rate

$$\chi^2 = \sum_k \frac{(f_k^{\text{exp}} - f_k^{\text{th}}(\Pi))^2}{\Delta_k^2} \quad (5)$$

with respect to the set of the *effective* parameters $\Pi = \{\tau_r, V_r, C, \alpha, \tau\}$. $\Delta_k = (\Delta f_k^+ + \Delta f_k^-)/2$ amounts to half the confidence interval for point k , with Δf_k^{\pm} given by Eq. 2. Because only five of the six parameters of the model neurons are independent (the response function Eq. 4 is invariant under the scaling $\theta \rightarrow \eta\theta$, $V_r \rightarrow \eta V_r$, $C \rightarrow C/\eta$ with $\eta > 0$), we set the threshold to $\theta = 20$ mV without loss of generality.

The minimum χ_{min}^2 of the quantity (5) with respect to the parameters set Π follows approximately a χ^2 distribution with $N-M$ degrees of freedom, where N is the number of experimental points, and $M = 5$ is the number of free parameters. The fit was accepted whenever the probability $P(\chi_{N-M}^2 \geq \chi_{\text{min}}^2)$ was >0.01 . An unequal variance t -test was used to detect differences in average neuron parameters (the same results were obtained with an equal variance t -test). Significance was taken at 5% level.

The input resistance of the neurons was calculated from the voltage transients in response to at least six different hyperpolarizing current pulses (600-ms duration, average of the last 300 ms; step amplitude: 20 pA). The membrane time constant τ was estimated by injecting brief (0.4 ms) hyperpolarizing current pulses (-2.5 nA) into the soma. From the averaged ($n = 50$) decaying voltage transient after this current pulse, τ was obtained from the slope of a straight line fitted to the tail portion of the semilogarithmic plot of the membrane voltage against time (Ianssek and Redman 1973). The membrane capacitance

was then obtained as the ratio between the membrane time constant and the input resistance. We refer to these values as to the *directly estimated parameters* in the following, as opposed to the *effective parameters* obtained from the fit of the model to the response functions.

Full model fit of the temporal response

The model neuron having the quasi-stationary firing rate given by Eqs. 3 and 4 is described by a single variable, the membrane voltage V , which below the spike threshold θ obeys

$$dV = -\frac{V}{\tau} dt + \frac{m_I - I_\alpha}{C} dt + \frac{\sigma_I}{C} \xi_t \sqrt{dt} \quad (6)$$

where $\sigma_I = s_I / \sqrt{2\tau_r}$ (symbols have the same meaning as in Eqs. 1 and 4). I_α is a feedback current driven by the neuron's instantaneous output rate

$$\frac{dI_\alpha}{dt} = -\frac{I_\alpha}{\tau_\alpha} + \bar{g}_\alpha \sum_k \delta(t - t_k) \quad (7)$$

where the sum is over all spikes emitted by the neuron up to time t . I_α can be interpreted as being (proportional to) the internal concentration of the ion species responsible for adaptation (see e.g., Powers et al. 1999; Sanchez-Vives et al. 2000; Sawczuk et al. 1997; Schwandt et al. 1989); \bar{g}_α as its peak conductance, and τ_α as its decay time constant to zero between action potentials. When $V = \theta$, a spike is said to be emitted, and V is reset to V_r , where it is clamped for τ_r ms. The output rate reaches eventually the quasi-stationary value given by Eq. 3 and 4 with $\alpha = \bar{g}_\alpha \tau_\alpha$ (for a comprehensive discussion of this model and its validation in the presence of noise, see La Camera et al. 2004a).

This model, with the neuron parameters as determined by the fit of the quasi-stationary response function (see the previous section), was used to fit the *instantaneous firing rate*, defined as the inverse of the ISI as a function of time, $f(t) = 1/\text{ISI}(t)$. For illustration purposes only, a smoothed version of $f(t)$, obtained by using a Savitzky-Golay polynomial smoothing filter (see e.g., Press et al. 1992) was used in Figs. 1–10. Note that the theoretical ISIs depend on the model neuron parameters $\Pi = \{\tau_r, V_r, C, \alpha, \tau\}$ (see *Data analysis and fitting procedure*). Including these as free parameters in the fitting procedure could have resulted in an over-fitting of the temporal properties. Moreover, neuron parameters should be the same, both after the response has reached its quasi-stationary characteristics, and during its temporal evolution. For this reasons, previously fitted neural parameters Π were held constant during the analysis of the temporal response. This limited the analysis to only those neurons with stable and fitted quasi-stationary response functions. Some of the PYR neurons studied by Rauch et al. (2003) could not be fitted according to the χ^2 test but were well described by the model in terms of average absolute difference between experimental and theoretical firing rates (<1.5 Hz per data point if the frequencies were <50 Hz, <2.5 Hz per data point for all the other frequencies). These neurons were included in the present analysis, giving a total number of $n_r = 92$ single recordings from $n = 21$ PYR neurons.

In most cases, one adapting current was not sufficient to reproduce the instantaneous firing rate, and two or more independent processes were required. In this more general model, I_α in Eq. 6 was the sum of independent components, $I_\alpha = \sum_k I_{\alpha_k}$, each of which obeying an equation like Eq. 7, with corresponding τ_k, \bar{g}_k such that $\bar{g}_k \tau_k \equiv \alpha_k$, and $\sum_k \alpha_k = \alpha$ (negative α_k s correspond to facilitating processes). This constraint ensures that the quasi-stationary firing rate of each spike train (reached when $t \gg \max_k \tau_k$) agrees with that given by Eq. 3. Note that it is necessary to consider the right number of processes to estimate the time constants involved because $\sum_{k=1}^n \bar{g}_k \tau_k = \alpha$, and this

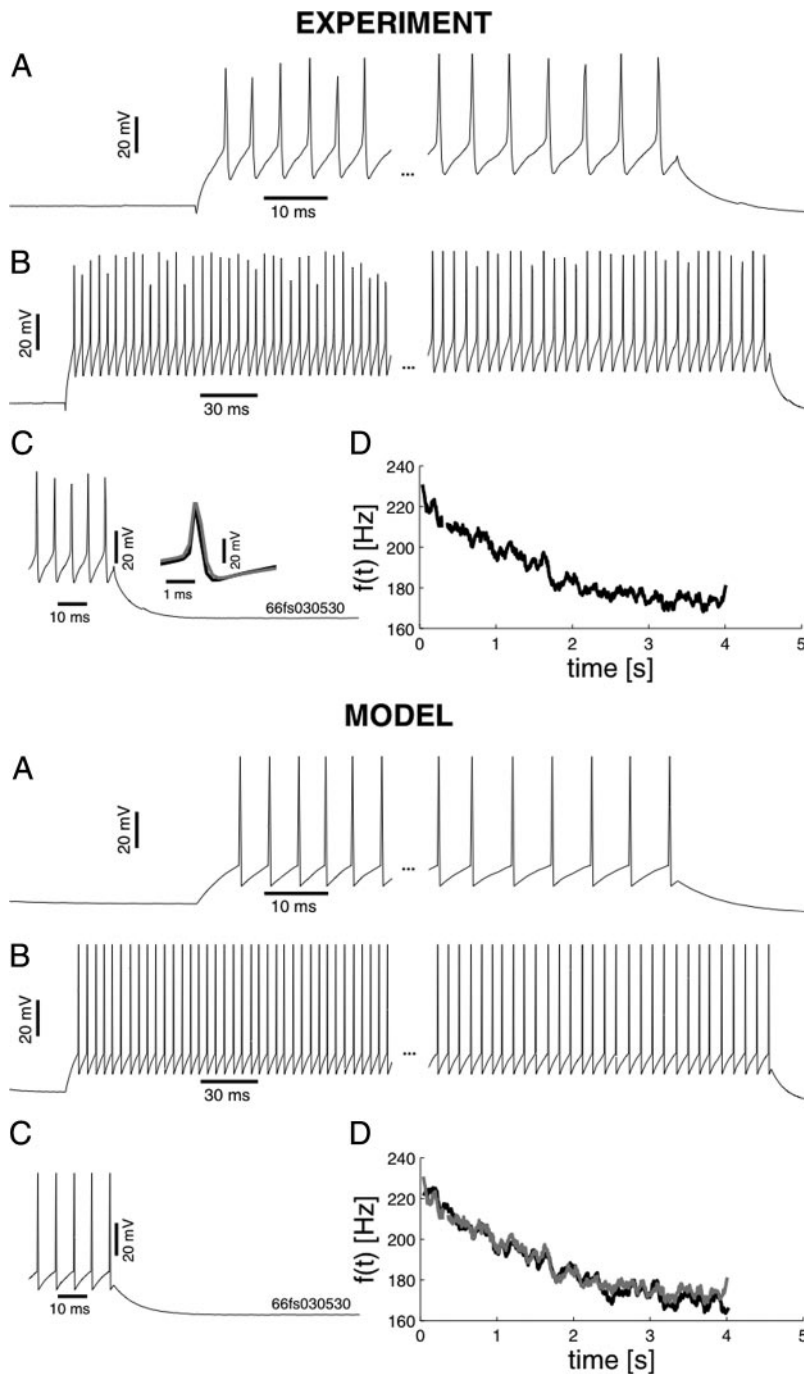


FIG. 1. The typical response of a L5 FS cell to a low-noise ($m_1 = 400$, $s_1 = 20$ pA) input current. *Top*: experimental data; *bottom*: model reproduction using the leaky integrate-and-fire (LIF) neuron. *A*: beginning and end of the spike train. No initial adaptation is visible, although the final part of the spike train clearly shows larger interspike intervals (ISIs; late adaptation). *B*: same as *A* with a different scaling. No initial adaptation is visible in the first 200 ms. *C*: end of spike train shows that there is neither slow afterhyperpolarization (sAHP) current after stimulus offset (*left*), nor difference in spike shape (DSS) between the average ($n = 20$) spike at the beginning (0.5 s, black) and at the end (3.6 s, gray) of stimulation (*right*). A longer recording time may reveal the presence of both (see e.g., Fig. 10). *D*: instantaneous firing rate $f(t)$ (see the text) shows the presence of slow adaptation [in MODEL, experimental $f(t)$ is in gray for comparison]. Neuron parameters are the best-fit parameters to the entire response function (including the adaptation parameter α): $\theta = 20$ mV, $V_r = 8.4$ mV, $C = 86$ pF, $\tau = 8.4$ ms, $\tau_r = 0$, $\alpha = 0.4$ pA \cdot s. The adaptation time constant τ_α remained undetermined by this fitting procedure and it was adjusted to match the time course of the spike frequency (MODEL, *D*). The value found was $\tau_\alpha = 2.2$ s and could be used to match the frequency time course of all other data points for this cell (see e.g., Figs. 2 and 7).

constraint will be satisfied with different values of τ_k depending on n , the total number of processes. The relative percentage of a process was defined as $\alpha_{k,\%} \equiv 100|\alpha_k| / \sum_{j=1,n} |\alpha_j|$. Unlike the neuron parameters, which were obtained from the fit to the quasi-stationary response and were therefore independent of firing rate, the parameters characterizing the temporal response were fitted separately for each recording and therefore were, at least in principle, firing-rate and/or input-current dependent. Their properties as functions of firing rate and input current are analyzed in detail in RESULTS.

The fit of the temporal response was achieved via a Monte Carlo procedure as described earlier (see *Data analysis and fitting procedure*), using as objective function the squared difference of the ISIs, i.e., $\chi_{\text{ISI}}^2 = \sum_j (\text{ISI}_j^{\text{exp}} - \text{ISI}_j^{\text{th}})^2$. $\text{ISI}^{\text{th}}(t)$ was obtained by simulating the

full IF model described in this section. The quality of the fit was assessed by eye and by comparison of the best value of χ_{ISI}^2 with the number of degrees of freedom $N-M$ (N is the number of ISIs in a given spike train and M is the number of parameters to be tuned, described in the following text). Most fits of the responses to step-like stimulation gave values of χ^2 around or less than $N-M$. This would make the fits acceptable if the errors on the single experimental ISIs, not available, would be around unity (in ms) (Press et al. 1992): a conservative value because it is comparable to the duration of an action potential. The (unknown) error in the ISIs would most likely be higher and hence the observed χ^2 smaller, making the test more significant. The exact reproduction of spike times, as assessed, e.g., through the Victor metric and similar spike train distances (see Victor 2005 for a review), was not the aim of the fitting procedure. Param-

eters to be tuned were the $\tau_k s$ ($\max n = 3$), the $\alpha_k s$ ($n - 1$, the n th being determined by $\alpha_n = \alpha - \sum_{k=1}^{n-1} \alpha_k$), plus one additional parameter, δm_I , representing a constant offset current. The input current to the model neuron was $I + \delta m_I$, where I was exactly the current injected during the experiment (i.e., the term $\delta m_I \cdot dt/C$ must be added to the right hand side of Eq. 6). [δm_I turned out to be different from zero only in PYR neurons to compensate for the strong burst-like initial adaptation which involves only the first one to three ISIs (most commonly a doublet of spikes, see RESULTS) (see also Rauch et al. 2003), not captured by model Eq. 7. This subtraction procedure compensates for the initial adaptation current in its steady state while neglecting the initial transient during the first few action potentials. No corrective term was required for fast spikers, consistent with the absence of strong initial adaptation in these neurons.]

The peak conductances \bar{g}_k were given by the ratio α_k/τ_k (negative if $\alpha_k < 0$, representing facilitation instead of adaptation). In total, this makes $M = 2n$ parameters to be fitted. For $n = 3$ processes (the maximum number of processes found to be required), $M = 6$. The number of ISIs (N) was in the range 300–600 for PYR neurons (30–60 Hz for 10 s); 400–800 (4 s) or 1,000–2,000 (10 s) for FS neurons (100–200 Hz). For each cell, four to eight different spike trains were analyzed, often with repetitions of the same input to compare intra-cell with inter-cell variability. The repetitions were never consecutive; FS neurons had typically a consistent response to the same stimulus, whereas PYR neurons would often display different time constants and amounts of the processes involved, although within the same order of magnitude. Most fits were obtained in case of step current stimulation, and then the best-fit parameters were used as the initial guess to fit the responses to noisy current.

Dependence of the adaptation/facilitation parameters on input current

Linear correlation of the adaptation/facilitation parameters $|\alpha_i|$ and τ_i (indicated generically with the symbol Y in the following), with output firing rate and input current (across all recordings of all neurons of the same type, i.e., either FS or PYR) was taken as a measure of the dependence of those parameters on output firing rate and input current, respectively. Because this analysis involved multiple comparisons, significance was taken at 0.5% level. The details of the analysis are reported in the APPENDIX. The dependence of Y on input current, $x \equiv m_I - I_{th}$, was then summarized either in the form of a linear relationship, $Y(x) = ax + b$ (if Y was positively correlated with x), or in the form of an exponential function, $Y(x) = ae^{-bx}$ (if anticorrelated with x), where a, b are constants. By interpolation, this provides the function $Y(I_+)$ for all input currents in the physiological range, where $I_+ \equiv I - I_{th}$. Parameters a and b were obtained through a standard least-square procedure. The functions $Y(x)$ were chosen because of the following observations: first, adaptation/facilitation can be observed only when the neuron is firing, hence it is more appropriate to describe them as functions of $m_I - I_{th}$ as opposed to m_I ; moreover, this avoids the problem of possibly having negative values of Y above rheobase, i.e., for $m_I > I_{th}$ (the parameters are positive by definition); second, increasing variables were, in the domain of interest, well described by their regression lines; and third, exponential curves provided fits almost as good as the regression lines to decreasing variables at the same time preventing them from reaching negative values at large inputs.

In the absence of correlation between Y and $x = m_I - I_{th}$, we summarized the statistical properties of Y by reporting the (combination of) truncated Gaussian distributions that approximate the experimental distribution. The Gaussian distributions were truncated at negative values because the parameters are positive by definition. Although it would be more appropriate to use a positive-definite distribution like, e.g., the Gamma distribution, in our data, there was little practical difference between the Gamma and the truncated

Gaussian distribution that approximates it, and for the sake of simplicity we chose the latter.

The experimental distributions shown in Fig. 8 were obtained by smoothing the data with a Gaussian filter at half the optimal bandwidth, to reveal features such as multiple modes (Bowman and Azzalini 1997). For the red curve in Fig. 8, *bottom right*, the optimal bandwidth was used. Correlations and other statistical analyses were performed on the raw data.

RESULTS

FS neurons response to in vivo-like input current

The response of $n = 15$ cells from the L5 of rat somatosensory cortex (P28-43) were collected using the random step protocol with fluctuating current described in METHODS. $n = 10/15$ were identified as FS cells, showed a consistent response function (see METHODS), and were further analyzed. A standard criterion for classification of cells as FS neurons was used (see e.g., Descalzo et al. 2005): short-duration of action potentials (< 0.5 ms), fast after-spike repolarization, absence of firing rate adaptation in the first milliseconds of the spike train, a steep frequency-current curve around rheobase (Figs. 1 and 4). We recorded also from $n = 12$ neurons in L2/3 (P16-27), 9 of which were clearly identified as FS cells as described in the preceding text. $n = 5/9$ neurons showed a consistent response function and were considered for further analysis. L5 and L2/3 interneurons had similar physiological parameters (i.e., *directly estimated* membrane time constant and capacitance, see METHODS and Table 1, *last 3 rows*), were injected with currents of similar magnitude and SD, and showed similar response patterns. As a consequence, their properties were summarized together unless explicitly noted.

Typical spiking patterns in response to prolonged (≥ 4 s) step- and noisy-current injections are shown respectively in Figs. 1 and 2. FS interneurons showed no initial adaptation (defined as a strong but transient decrease in firing rate that involves the first few spikes only) in accord with what reported in previous studies (e.g., McCormick et al. 1985). Nevertheless, the cells showed consistent slow reduction in firing rate over time for stimuli longer than a few hundred milliseconds, see Fig. 1, *A* and *B* (experiment). This behavior is well captured by the simple adapting model described in METHODS (Eqs. 6 and 7; Fig. 1, model) with an adaptation time constant $\tau_\alpha = 2.2$ s. The presence of slow adaptation in FS neurons has been reported only recently by Descalzo et al. (2005) in ferret visual cortex, both in vitro and in vivo; preliminary evidence in rat somatosensory cortex in vitro had been reported by Reutimann et al. (2004).

In a fraction ($n = 5/15$) of interneurons one adapting process was not enough to capture the time course of the firing rate, and the generalized model described in METHODS had to be used. Two components were sufficient to reproduce the data, one with a time constant of $\tau \sim 100$ –300 ms, the other slower and spanning a large range of time constants ($\tau \sim 0.8$ –30 s). Nine cells of 15 showed *stuttering* behavior (see Fig. 5, *left, inset*), in response to low noise current ($s_I = 0$ –30 pA). Such behavior was consistently suppressed in the presence of higher input fluctuations ($s_I = 50$ –200 pA) as found for PYR neurons (Rauch et al. 2003). A more detailed analysis of the temporal properties of the response will be reported in later sections.

Due to slow adaptation, the firing rate either reached an almost constant value during the last segment of stimulation (quasi-stationary response, see METHODS) or continually declined in a linear-like fashion until the end of stimulation (nonstationary response), depending on the neuron and on the strength of the input. This was quantified by the index $\delta f = (f_{\text{init}} - f_{\text{final}})/\delta T$ (see METHODS), which provided a measure of late (or slow) adaptation. For the sake of subsequent analysis, nonstationary responses were considered as quasi-stationary if their inclusion in the fitting procedure described in *Data analysis and fitting procedure* did not alter the outcome of the fit (see also the next section). Typically, in FS interneurons this happened for δf smaller than ~ 5 Hz/s (~ 10 Hz/s in a few L2/3 interneurons) at maximal frequency (150–200 Hz); in PYR cells, for $\delta f = 1$ Hz/s at maximal frequency (40–60 Hz). Hence the decrease in firing rate over time after the initial transient was much more pronounced in FS cells than in PYR neurons (see also Fig. 6). In $n = 10/15$ interneurons, δf values were strongly correlated with the quasi-stationary output rate f ; in eight of these neurons, correlations were strong but significant only at low values of s_I (Pearson ρ and Kendall's tau, $P < 0.05$). Note that although a large amount of noise typically weakened the correlation between δf and f , it did not decrease the amount of maximal adaptation (quantified by the maximal δf).

IF reduction of FS interneurons

The response function of the modified LIF neuron was fitted to the response of consistent cells as described in METHODS. A high percentage of cells could be fitted in both L5 and L2/3. Results are summarized in Table 1, where also the effective parameters for PYR neurons taken from Rauch et al. (2003) are reported. A few examples are shown in Fig. 3. L5 and L2/3 FS neurons differ significantly in the (effective) capacitance C (smaller in L5), the membrane resistance R (larger in L5), and in the rheobase current I_{th} (smaller in L5). These differences could in part be accounted for by the different age of the rats in the two groups. It is interesting to note that although the directly estimated C , τ , R had similar values for L5 and L2/3 FS neurons, the effective C , R were the *only* parameters which were significantly different between L5 and L2/3 FS cells (t -test, $P < 0.05$). A discrepancy between directly estimated and effective parameters was found also in PYR neurons (Rauch et al. 2003).

Comparison between the response functions of FS and PYR neurons

The “average” response functions of PYR and FS neurons are shown in Fig. 4, where the average best-fit parameters from Table 1 were used. The maximal amount of noise which could be used for FS interneurons was $s_I = 200$ pA, as opposed to 500 for pyramids. However, the response at rheobase for the maximal s_I used (~ 50 Hz) was stronger than for PYR neurons (~ 10 Hz). This can be attributed to a significantly smaller membrane time constant in FS neurons (Table 1; t -test, $P < 0.002$), mostly due to a smaller membrane capacitance. Moreover, because of a larger input resistance, FS neurons have a smaller rheobase current. Taken together, these factors imply that FS neurons respond faster and to a much higher extent to

any kind of change in the input than PYR neurons. Consistently, FS cells had smaller effective C , τ , and τ_r , than PYR neurons (Table 1).

Note that α is smaller in FS neurons, despite the larger index δf quantifying slow adaptation (1 Hz/s for pyramids vs. 5–10 Hz/s for fast spikers). This is the consequence of the steeper slope of FS cells' response function (Fig. 4). Indeed, to quantify adaptation, both α and the slope of the response function are required. According to Eq. 3, where the *non*-adapted response function Φ appears, the adapted firing rate f is given by the nonadapted response at $m_I' = m_I - \alpha f$, so that a steeper response function requires a smaller value of α to produce the same amount of adaptation. In Fig. 3, one can notice that the α values are indeed anticorrelated with the slopes of the corresponding response functions. The results of this section point to a faster and larger response of FS neurons to in-vivo-like current, compared with PYR neurons.

Variability of the ISIs

We also measured the ISI variability of FS neurons in response to in-vivo-like current, through its coefficient of variability (CV, see METHODS). Strictly speaking, this measure can be meaningfully applied only to stationary spike trains (Gabbiani and Koch 1998). Given the presence of several temporal processes, the CV was calculated on the portion of spike train left after the removal of the first 500 ms, an initial transient of the duration of the faster adaptation/facilitation processes (see the next section and Table 2 for details). This allows us to deal with the variations due to slow adaptation of the firing rate only. Two typical cases are shown in Fig. 5 for one L5 (*left*) and one L2/3 (*right*) FS interneuron, together with the prediction of the LIF model neuron the parameters of which were tuned to fit the firing rates only (full lines). Only one adapting current was used in the model Eqs. 6 and 7. The use of more adapting/facilitating components to fit the temporal response did not significantly improve the match to the CV (not shown). In the model with one adaptation component, the CV slightly increases with τ_α up to $\tau_\alpha \sim 500$ ms, which was the value used in Fig. 5 to get the best match with the data. This type of behavior is expected for τ_α larger than the membrane time constant (Liu and Wang 2001). Above $\tau_\alpha = 500$ ms, no change in variability was observed.

FS neurons show variable spike trains in response to in-vivo-like current, even for small input fluctuations and large output rates. The uppermost curve in the *left panel* was obtained in response to current with $s_I = 150$ pA and the CV was of the order of (or larger than) 0.6 for all output frequencies (up to $f = 200$ Hz). In the 20- to 50-Hz output range, the level of ISI variability in FS neurons is close to what found extracellularly and intracellularly in vivo in many areas of the cortex of different animal species, (e.g., Gershon et al. 1998; Gur et al. 1997; Holt et al. 1996; Lee et al. 1998; Shinimoto et al. 2003, 2005; Wiener et al. 2001). For larger output rates (≤ 200 Hz), the coefficient of variability drops to values that are still > 0.5 , if there is enough variability in the input. High ISI variability in the intact brain is believed to be the result of a balanced synaptic input current, characterized by large fluctuations around a sub-threshold average (e.g., Amit and Brunel 1997; Destexhe et al. 2001; Haider et al. 2006; Holt et al. 1996; Lerchner et al. 2006; Shadlen and Newsome 1994, 1998; Shu

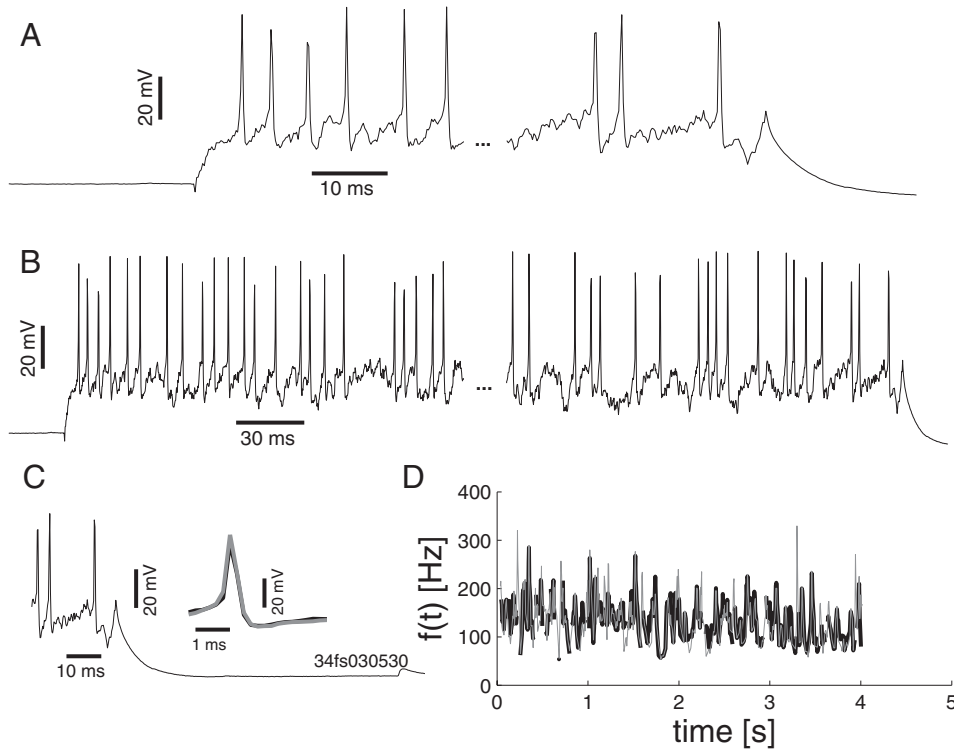


FIG. 2. The typical response of a L5 fast spiking (FS) cell to a high-noise ($m_1 = 300$, $s_1 = 150$ pA) input current. The plots are as in Fig. 1. *D*: instantaneous frequency of the model is plotted in gray (same parameters as in Fig. 1).

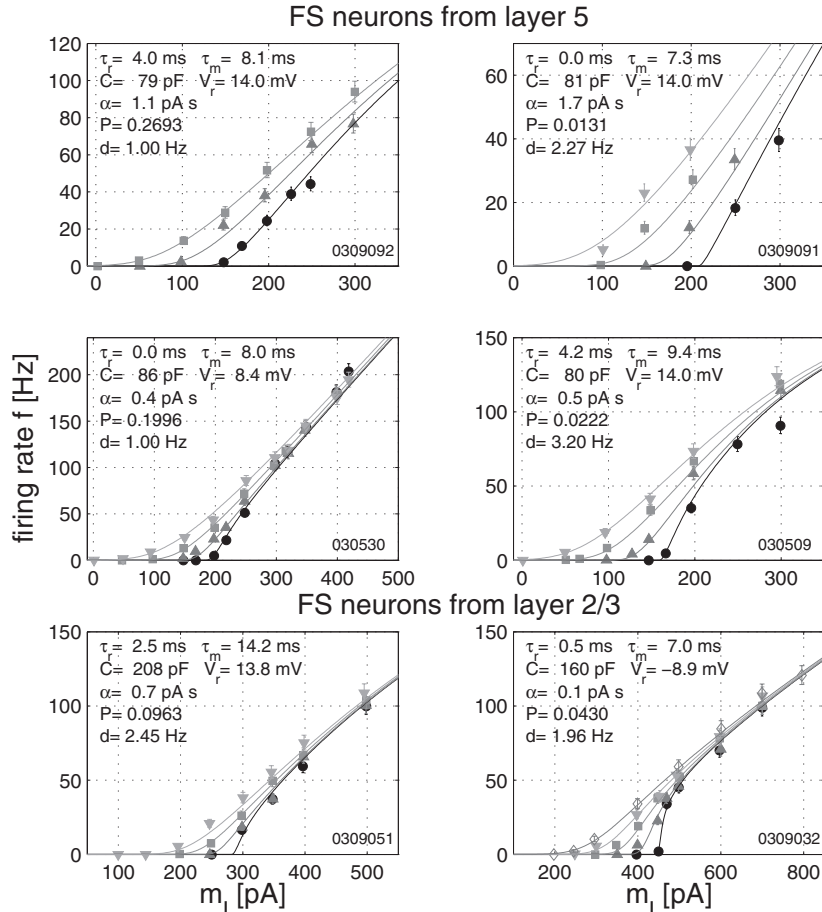


FIG. 3. Fit of the LIF model response function to the experimental response of FS interneurons. Shown are 4 examples from L5 (*top*) and 2 from L2/3 (*bottom*). Symbols are experimental quasi-stationary firing rates, full lines are the model fits to the data (Eqs. 3 and 4). Error bars are the confidence intervals of Eq. 2. The output rates are plotted against input current, m_1 , for different values of the input fluctuations, s_1 . Each curve corresponds to a constant value of s_1 , which in pA were (clockwise from *top left panel*; from right- to left-most curve in each plot): (50,100,150); (10,50,100,150); (10,50,100,150); (10,50,100,150,200) (*bottom right*); (10,50,100,150) (*bottom left*); (20,50,100,150). The best fit parameters (defined in METHODS) are reported in the left top corner of each plot. P is the probability that a χ^2 variable with the same number of degrees of freedom is larger than the best-fit one. A fit was accepted if $P > 0.01$. d is the absolute discrepancy, i.e., the average (across all points) absolute difference between the measured and the theoretical frequencies of the best-fit curves.

TABLE 1. *LF neuron effective parameters*

	FS, L5	FS, L2/3	PYR, L5
$\alpha, pA \cdot s$	0.8 ± 0.5	1.0 ± 0.9	10.8 ± 6.3
τ_r, ms	1.4 ± 2.1	3.3 ± 2.6	9.4 ± 6.5
V_r, mV	8.8 ± 9.4	5.3 ± 11.3	9.9 ± 10.2
τ, ms	7.5 ± 1.5	8.3 ± 3.6	26.3 ± 13.2
C, pF	$80 \pm 13^*$	$140 \pm 48^*$	530 ± 290
$R, M\Omega$	$95 \pm 14^*$	$59 \pm 10^*$	50 ± 10
I_{rh}, pA	$216 \pm 30^*$	$351 \pm 66^*$	410 ± 70
τ_{de}, ms	14.2 ± 1.7	12.7 ± 1.0	23.8 ± 2.5
C_{de}, pF	150 ± 30	135 ± 38	890 ± 150
$R_{de}, M\Omega$	98 ± 22	99 ± 20	27 ± 5

Summary of the results of the fit of the leaky integrate-and-fire (LIF) neuron response function (Eqs. 3 and 4) to the experimental response functions of fast spiking (FS) interneurons (6 fits of 10 interneurons from L5 and $n = 5/5$ fits to neurons from L2/3) and pyramidal (PYR) cells ($n = 4/14$ from L5) from acute slices of rat somatosensory cortex. Values are shown as means \pm SD across fitted neurons (see METHODS for a definition of the neuron parameters). The last three rows show directly estimated (*de*) parameters. The threshold for spike emission was held fixed to 20 mV (see METHODS). The parameters for PYR cells (rightmost column) are taken from Rauch et al. (2003). *, visual aid to quickly detect significant differences between L5 and L2/3 FS ($P < 0.05$, *t*-test). Rats' ages were (post-natal days) $37 \pm 6^*$ (FS, L5), $22 \pm 4^*$ (FS, L2/3), and 27 ± 3 (PYR, L5).

et al. 2003; van Vreeswijk and Sompolinsky 1996). Comparison between the cases of small and large input fluctuations in the data of Fig. 5 supports this view.

It is also interesting to compare this result with the typical variability of a L5 PYR neuron (dashed lines in *left panel*). The maximal CV is <0.5 even though $s = 300$ pA was used (for $s = 400$ pA, $CV \sim 0.6$, but only for $f < 30$ Hz) (see Rauch et al. 2003). As opposed, for the L5 FS cell in the left panel, $CV \sim 0.8$ for $f \sim 80$ Hz, the maximal stationary firing rate found for a L5 PYR neuron. These results are consistent with the higher sensitivity to fluctuations found in FS neurons compared with PYR neurons. Interneurons in L2/3 tend to be less variable than in L5, especially around maximal frequency (typically $CV \sim 0.5$ compared with ~ 0.6 for inputs with maximal s_i). A few spike trains in response to low-noise input showed high variability due to stuttering behavior (Fig. 5, *inset*), that cannot be reproduced by the model.

Dynamics of the response: adaptation/facilitation of the firing rate

So far we have been concerned with the properties of the quasi-stationary response as reached after prolonged exposure

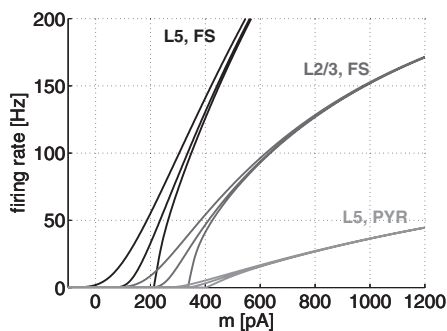


FIG. 4. Comparison between the quasi-stationary response of FS and PYR cells. The steady state responses were obtained using the average best-fit parameters of Table 1. Response functions plotted as in Fig. 3, with $s_i = 0, 100, \text{ and } 200$ pA.

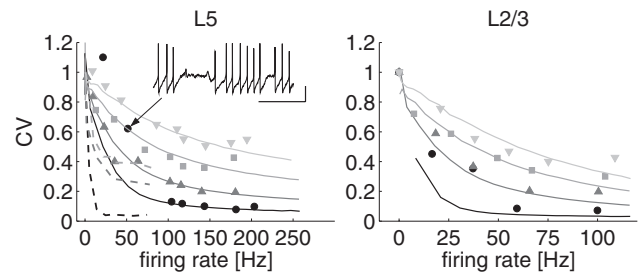


FIG. 5. Coefficient of variability (CV) of the ISIs in response to in-vivo-like current for 2 FS neurons (symbols) vs. output rate (CV-f curves), together with the prediction of the LIF model (full lines). On each curve s_i is held constant while m_i is swept along. The parameters of the model were tuned to fit the firing rates only. The CV of LIF model was obtained for each point from a 500-s simulation of the model, Eqs. 6 and 7 (after discarding a transient of 5 s). Adaptation time constant $\tau_\alpha = 500$ ms in both cases (the CV did not change appreciably above this value, see the text). *Left*: L5 cell ($s_i = 20, 50, 100, \text{ and } 150$ pA); *Right*: L2/3 cell ($s_i = 10, 50, 100, \text{ and } 150$ pA). Dashed lines in *left panel* show the typical CV-f curves of a L5 PYR neuron for comparison ($s_i = 0, 200, \text{ and } 300$ pA). *Inset*: segment of the voltage trace for the point indicated by the arrow (calibration bars: 100 ms and 20 mV).

to a stationary stimulus, and only mentioned in passing the temporal dynamics through which the quasi-stationary behavior was reached. In this section, we characterize the dynamic processes involved, summarizing some of their statistical properties.

PYR and FS neurons showed different temporal patterns in response to a sustained input with stationary statistics. A comparison is shown in Fig. 6. Note the phasic response of the PYR neuron, characterized by an extremely fast and strong initial adaptation, followed by an increase in firing rate, and then by a slow decay. FS interneurons lacked the strong initial phase, and were characterized by tonic firing, although of slowly decreasing rate over time. To capture these behaviors, we extended the model IF neuron to include a minimal number n_p of independent processes, sufficient to characterize the temporal response. In order for the extended model to have the same quasi-stationary firing rate as the original model used to fit the response functions of Fig. 3, the same neuron parameters were used, including $\alpha = \sum_i \alpha_i$ (see *Full model fit of the temporal response*). This left $n_p - 1$ independent α_i and their time constants to be adjusted by fitting the instantaneous firing

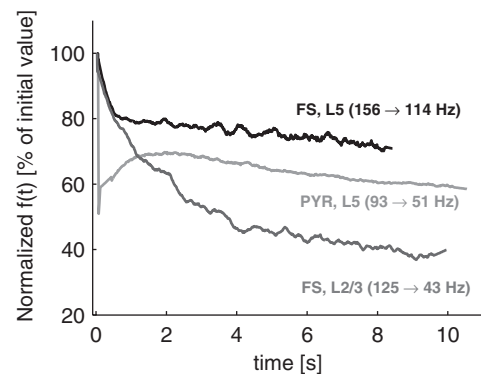


FIG. 6. Comparison between the temporal response of FS and PYR cells. The figure shows 3 examples of firing rate activity as a function of time, normalized to the inverse of the 1st ISI (the actual initial and final firing rates are reported in the figure). Shown are: a L5 FS that can be fitted with 2 processes (time constants of 220 ms and 3.6 s), a L2/3 FS (1 process, $\tau = 15$ s), and a PYR neuron (3 processes, time constants of 43 ms, 920 ms and 2.9 s). Note that the time constants might look more similar than they are because the firing rates converge to different steady-state values.

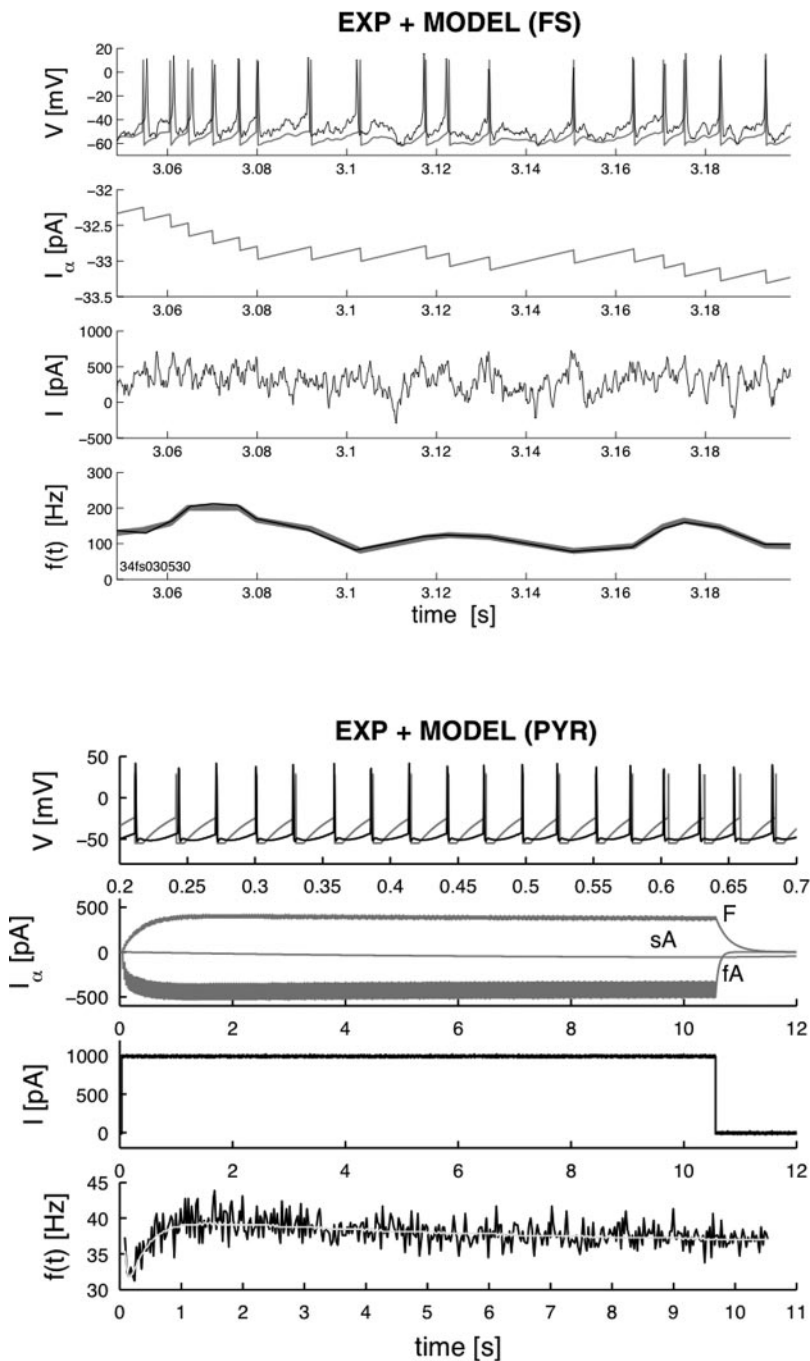


FIG. 7. Examples of the fitting procedure of the temporal response for a L5 FS interneuron (*top*) and a PYR neuron (*bottom*). Shown (from top to bottom in each panel) are the membrane potential, the adaptation current (Eq. 7), the total input current, and the instantaneous firing rate. The input current is the same as injected into the neuron. The LIF model is reported in gray, the experimental data in black. *Top*: details of the fit of the response of the FS interneuron shown in Fig. 2, which can be obtained with a single process of slow adaptation (time constant of 2.2 s). *Bottom*: a typical example of the response of a PYR neuron to step-current stimulation, together with its model best-fit. Note the presence of facilitation (F) and 2 adaptation processes, 1 fast (fA, time constant of 58 ms, representing 47% of the adapting/facilitating components), the other much slower (sA, 6.3 s, 9%). The facilitating process had a time constant of 230 ms. Note the different time scales between *top* and *bottom* panels.

rate. Two examples of this fitting procedure are shown in Fig. 7, for a noisy-driven L5 FS cell (*top*) and a step-driven PYR neuron (*bottom*). A summary of the results is reported in Table 2.

No more than two processes were needed for FS interneurons (the fast and slow adapting processes mentioned in a previous section), whereas three to four processes were required for PYR neurons, to which we will refer as (from faster to slowest) *initial adaptation* (iA, affecting the first few ISIs only), *fast adaptation* (fA, $\tau \sim 50\text{--}200$ ms), *early facilitation* (F, $\tau \sim 0.5\text{--}1$ s), and *slow (or late) adaptation* (sA, order of seconds). The adaptation/facilitation components became clearly visible above a critical firing rate, ~ 30 Hz for PYR neurons (all processes) and above ~ 40 Hz (sA) or 80 Hz (fA)

for FS interneurons (with no difference between L5 and L2/3). We next discuss their properties in turn.¹

INITIAL ADAPTATION. *Initial adaptation* (iA), defined as a *burst-like* adapting process affecting only the first one to three ISIs (Rauch et al. 2003; Sawczuk et al. 1997), was present in 13/21 PYR neurons [$n_r = 15$ recordings, across which initial frequency was $f_i > 52 \pm 24$ (SD) Hz, with a minimal value of $f_i = 17$ Hz], and absent in FS neurons. The model Eq. 7 is inadequate to describe iA, therefore we used

¹ The values reported in the text are taken from data biased toward high output rates to have as many processes as possible in each recording. This means that the minimal frequency reported for a given process could be larger than the actual *critical* frequency required for the process to be observed.

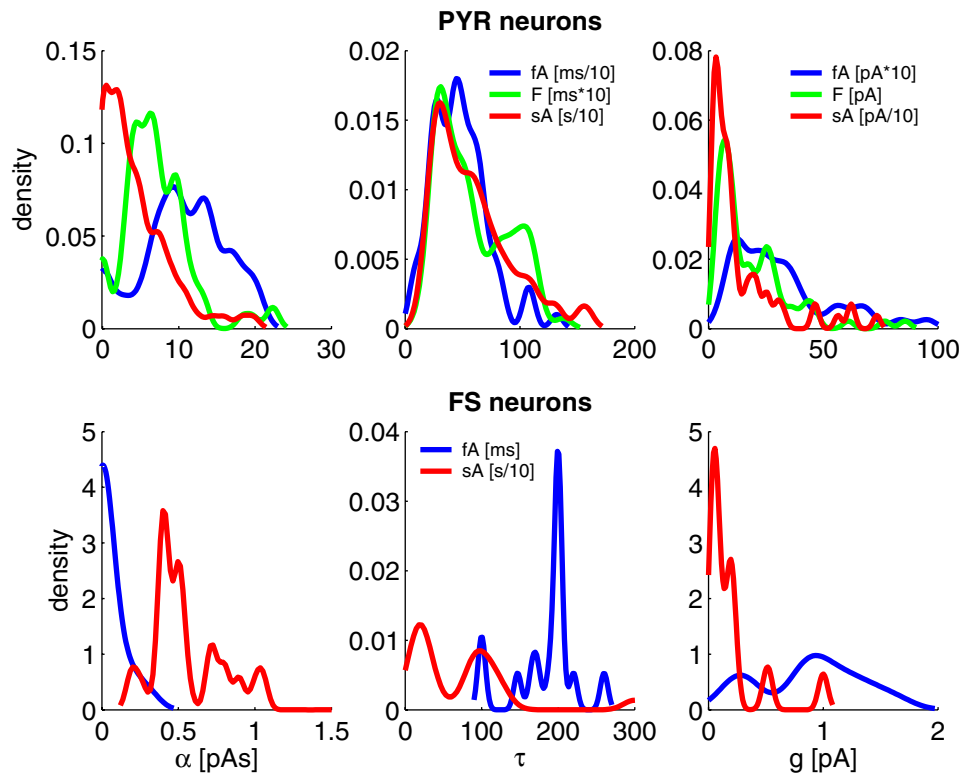


FIG. 8. Distributions of the parameters characterizing the temporal response of PYR and FS neurons. \bar{g} and τ defined as in Eq. 7, with $\alpha = \bar{g}\tau$ for each process. fA, fast adaptation (blue); F, early facilitation (green); sA, slow adaptation (red). Note the different units for different processes in panels provided with a legend.

a constant offset current δm_j , which activates immediately after the onset of the stimulus (see *Full model fit of the temporal response*).

FAST ADAPTATION. *Fast adaptation* (fA). Fast- and slow-duration adaptation mechanisms are well documented in the literature on PYR neurons but only recently were reported in FS neurons (Descalzo et al. 2005; Reutimann et al. 2004). The longest time constants of fA were 132 ms (PYR) and 260 ms (FS), whereas the shortest time constant of sA was ~ 1 s in all cells. The two distributions were clearly separated around the value of 0.5 s, which was then used to discriminate fA from sA. Fast adaptation was slower in FS neurons compared with pyramids, $\tau_{fA} \sim 200$ (FS) versus 50 ms (PYR), see Table 2; was always present in PYR neurons, while present only in $\sim 30\%$ of interneurons (for output rates larger than ~ 80 Hz), where it contributed $\sim 30\%$ of the total adaptation (vs. $\sim 50\%$ in PYR neurons, see Table 2).

SLOW ADAPTATION. Slow adaptation (sA) was present in all neurons, for output rates larger than ~ 30 Hz (PYR) or ~ 50 Hz (FS). In PYR neurons, sA spanned a unimodal range of time constants, 1.4–15.7 s ($n = 17/17$ cells, $n_r = 66$ recordings), peaked around 6 s (see Fig. 8). In FS interneurons, sA spanned a bimodal range of time constants (mostly in the range 0.8–15 s, with $\tau \sim 30$ s in a few cases; $n = 14/14$, $n_r = 60$), peaked around $\tau_{sA}^{(1)} \sim 2$ and $\tau_{sA}^{(2)} \sim 12$ s, respectively (see Fig. 8 and Table 2). This suggests that sA in FS neurons could be divided further into two processes. We will take this possibility into account in a later section, when attempting a model of the dependence of sA on input current.

EARLY FACILITATION. *Early facilitation* (F) manifests itself with a progressive shortening of the ISIs during, approximately, the first second of stimulation, after which the ISIs either remain constant or start to increase steadily (signature of

sA), sometimes until a new plateau has been reached (quasi-stationary points). Facilitation was found in all PYR neurons, but in none of the FS neurons. The time constant of the process ranged from a few hundreds milliseconds to ~ 1 s ($n = 17/17$, $n_r = 77$), and accounted for 37% of the adaptation/facilitation processes, with an extended range (12–100%; see Table 2). Purely facilitating spike trains were observed at low frequencies, 20–30 Hz, where neither iA nor sA made an observable contribution ($n = 2$ neurons). Facilitation was found also at high initial rates (≤ 120 Hz), where both iA and sA were strongly present. All three processes were present if the output rate was above a critical value ~ 30 Hz, as in Fig. 7, *bottom* (occasionally, also at lower output rates). In such cases, the spike train toward the end of stimulation was typically adapted, evidencing a larger effect of adaptation versus facilitation on the final output rate. F was present also when other pipette solutions were used, i.e., in the presence of 135 mM of K-methylsulfate, or in the presence of 10 mM EGTA, with similar time constants (Rauch et al. 2003). In both PYR and FS neurons, there was occasionally evidence of a delayed response of the first action potential after stimulus onset, especially for stimulus strength around rheobase. Such a behavior is to be kept distinct from facilitation, given the absence of (transient) monotonic decrease of ISI duration after the onset of the delayed response.

A few outlier cells had atypical behavior and were not included in the analysis of Table 2. Instead of sA, two PYR neurons had *slow facilitation* ($\tau > 20$ s), whereas a third neuron had two components of faster adaptation ($n_r = 4$ recordings); moreover, facilitation was rare in this neuron, and visible only at an unusually large initial firing rate of 100 Hz. One L2/3 FS cell showed intermediate-duration adaptation of 500 ms.

TABLE 2. Summary of the temporal properties of the response of FS and PYR neurons

	FS	PYR
τ_{fA} , ms	180 ± 40 [100–260]	48 ± 25 [6–132]
τ_F , ms	—	580 ± 300 [125–1380]
$\tau_{sA}^{(1)}$, s	2.1 ± 0.9 [0.8–5]	5.8 ± 3.4 [1.4–15.7]
$\tau_{sA}^{(2)}$, s	12.1 ± 6.2 [7.3–30]	
α_{fA} (%)	31 ± 14 [5–58]	52 ± 16 [15–79]
α_F (%)	—	37 ± 19 [12–100]
α_{sA} (%)	92 ± 15 [42–100]	23 ± 18 [4–45]

$\alpha_{\%}$ is the relative contribution of each process. $100 |\alpha_k| / \sum_j |\alpha_j|$ (see METHODS, *Full model fit of the temporal response*), whereas τ is the time constant of the corresponding process (note that there are 2 τ_{sA} for FS interneurons, because the distribution of this time constant was bimodal, see Fig. 8). Results are reported as means ± SD, with ranges reported in square brackets. The median was always very close to the mean and was not reported in the table. Recordings with sA only were found in 10 out of 14 interneurons (for a total of 55 recordings from which the parameters of this table were estimated); 4 of 14 interneurons had recordings with fast and slow adaptation (15 recordings); all PYR neurons (17/17) displayed the pattern fA-F-sA (77 recordings). See also the text. fA, fast adaptation; F, facilitation; sA, slow adaptation.

Interaction between the adaptation/facilitation processes

For both FS and PYR neurons, the percentages of the three processes (fA, F, and sA) were mutually (i.e., pair-wise) anticorrelated (for example, for PYR neurons $\rho \leq -0.4$, $P \leq 10^{-3}$): the more of one process, the less of the others. In PYR neurons, the higher the output rate, the more (and faster) sA, the less (and slower) F, whereas fA did not depend on firing rate (see the APPENDIX for details). At high firing rates, sustained activity was overtly affected by slow adaptation. As opposed to PYR neurons, no clear relation to firing rate emerged in FS neurons. The $\alpha_{\%}$ s were not correlated with output rate, and no pairwise correlations were found among the sA parameters, whether the time constants were considered separately ($\tau_{sA}^{(1)}$ and $\tau_{sA}^{(2)}$) or not (see the previous section). Recordings with larger output rates had a tendency to be dominated by sA, with less (but faster, as opposed to PYR neurons) fA.

Effect of input fluctuations on adaptation

In FS neurons, neither fA nor sA were correlated with average input current (either m_I or $m_I - I_{th}$; details are deferred to the next section). However, fast adaptation was found only in the presence of small fluctuations ($s_I < 60$ pA), whereas slower adaptation was just as strong irrespective of input fluctuations. This suggests that the input fluctuations play a role in selecting the type of adaptation taking place, independently of average input current (for each s_I , the same spectrum of m_I values were used). However, there was no clear relationship between the amount of fA and the value of s_I (not shown).

We found no evidence of a similar effect in PYR neurons. In the presence of large input fluctuations, the clear phasic response of Figs. 6 and 7 is more difficult to make out, but initial adaptation was still perceivable (data not shown). A comparison of the duration of the first few ISIs compared with the subsequent few ISIs, in the presence and in the absence of fluctuations, showed no appreciable difference in the two conditions, pointing to the presence of the same temporal processes in both cases. Specifically, we counted the number n_1 of ISIs in the first 100 ms (the order of magnitude of duration

of fA), calculated their cumulative duration T_1 , and compared T_1 with the cumulative duration T_2 of the same number n_1 of subsequent ISIs. A spike train was considered fast adapting if $T_1 < 0.75 T_2$ (a conservative measure, aimed at preventing taking into account spikes due to the occasional excess of upward deflections of the input current in the first 100 ms). For each cell, we compared the fraction of fast-adapting spike trains obtained in response to fluctuating and constant stimuli, respectively. These fractions were similar in all of the analyzed neurons and were sometimes larger in case of fluctuating inputs, leading to the conclusion that our data do not support a strong, general effect of input fluctuations on fast adaptation in PYR neurons. Moreover, the slow adaptation index δf had its maximal value unaffected by fluctuations, and early facilitation was observed in all recordings. In summary, input fluctuations did not disrupt the cellular properties of adaptation/facilitation in PYR neurons.

Dependence of adaptation/facilitation on input current

In this section, we report how adaptation/facilitation relate to input current. In the following, we indicate with the symbol Y the generic parameter τ_i or α_i . A dependence of Y on input current was inferred if Y was linearly correlated with $m_I - I_{th}$ (across all recordings of all neurons of the same type, see METHODS). Two examples of correlations are shown in Fig. 9. The details of the correlation analysis are reported in the APPENDIX.

If Y and $x \equiv m_I - I_{th}$ were positively correlated, the regression line, $Y(x) = ax + b$, was used to describe the dependence of Y on x , whereas an exponential function, $Y(x) = ae^{-bx}$, was used in case of anticorrelation, mainly to avoid negative values of the parameters for large input currents (see METHODS for details). The effect of initial adaptation in PYR neurons, affecting only the first 1–3 ISIs, was taken into account by a corrective term δm_I , as explained in *Full model fit of the temporal response*. δm_I [-200 ± 210 pA, range (-800 , 480) pA] was negatively correlated with $m_I - I_{th}$ (-0.263 , $P = 0.016$), and we chose a linear model for it as there was no need to prevent negative values. The results are summarized in Table 3, where models are reported as $Y(x) \pm CV_Y$, where $Y(x)$ expresses parameter Y as a function of input current x , and CV_Y is its coefficient of variability (SD/mean). CV_Y gives a measure of the variability found across different recordings and different neurons.

In Table 3, $G(\mu, \sigma)$ stands for truncated Gaussian distribution with mean μ and SD σ , and represents the best Gaussian approximation to the experimental distributions (Fig. 8) of those parameters not correlated with input current (see METHODS and the APPENDIX for details of the analysis). This was the case for all adaptation parameters in FS interneurons. In particular, τ_{sA} 's distribution had two peaks of similar magnitude and was well approximated by a linear combination of two Gaussian distributions (Table 3).

A model of adaptation in FS neurons should also take into account that fA was present only in 30% of the cells and disappeared for $s_I > 60$ pA, whereas sA was always present. The peak of the α_{fA} distribution could be made dependent on s_I , so to vanish for large input fluctuations. However, no simple monotonic relationship between the amount of sA and s_I was found in the data.

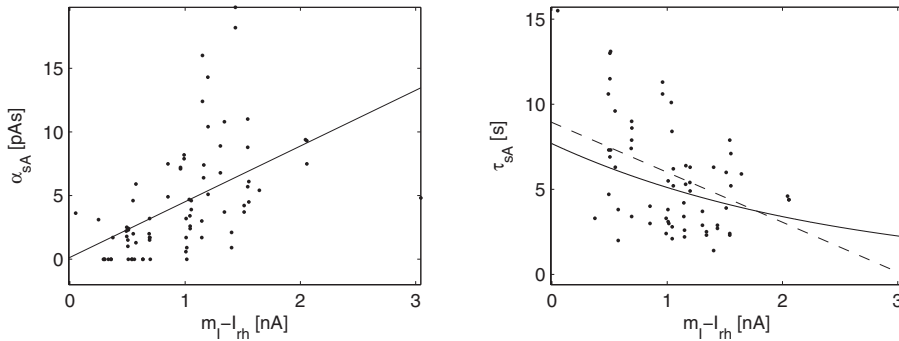


FIG. 9. Example of input-dependent models: α_{sA} (left) and τ_{sA} (right) for PYR neurons. Best-fit parameter values (dots), their regression lines (straight lines) and their models (full lines) are shown. For α_{sA} , the regression line is also the model (as reported in Table 3); for τ_{sA} (right), the model is the exponential curve (full line). Linear correlations are 0.53 ($P < 10^{-5}$; left) and -0.51 ($P = 0.0001$; right).

Finally, one may look for a generalization of the relationship $Y = Y(x)$ in the presence of a slow time-varying mean current $x(t)$ (slow enough that the assumption of quasi-stationarity is not substantially violated). The easiest generalization would be a first-order dynamical approach to $x(t)$, as in $\tau_Y(dY/dt) = -Y + Y[x(t)]$, with τ_Y a suitable time constant and $Y(x)$ given by Table 3. We could not test this hypothesis because we stimulated the neurons with stationary current only (i.e., with current of constant mean and variance). However, we checked with simulations that an instantaneous dynamics $Y(t) = Y[x(t)]$ results in a time course of the instantaneous firing rate which is indistinguishable from that produced by the first-order dynamics.

DISCUSSION

We studied in detail the firing patterns of FS and PYR neurons from rat neocortex in response to prolonged stimulation with in-vivo-like input current. In the first part of this paper, the quasi-stationary response of FS neurons (both the average firing rate and the variability of the interspike intervals) was characterized as a function of the average and the SD of the Gaussian input current and compared with the response of PYR neurons, previously studied with the same protocol (Rauch et al. 2003). This was a necessary step to study, in the second part of the paper, the temporal properties of the response of FS and PYR neurons. Several processes were found

to underly the time course of the instantaneous frequency, which could be reduced to a small number (1–4) of phenomenological mechanisms. A LIF neuron model, endowed with such mechanisms, reproduces the observed temporal response. The distributions of the temporal parameters (across all recordings of all neurons of the same type) are broad (Fig. 8) and cover several time scales, ranging from a few milliseconds to several seconds, suggesting that a continuum of time scales could be represented in the firing patterns of FS and PYR neurons, also in response to stationary stimuli and in the presence of input fluctuations.

Comparison between FS and PYR neurons

FS neurons differ from PYR neurons in several ways. The slope of the response function was steeper in FS neurons, 200–1,000 Hz/nA as opposed to ~ 50 Hz/nA for PYR neurons with a maximal firing rate ≤ 200 Hz (FS) versus 60 Hz found in pyramids (Fig. 4). FS interneurons were more sensitive to input fluctuations: s_I as small as 150 pA was able to elicit $f = 50$ Hz at rheobase for FS cells, but < 15 Hz in PYR neurons (Fig. 4). Moreover, at parity of input fluctuations and output firing rate, the CV of the ISIs is more than twice as large in FS interneurons (~ 0.7) compared with pyramids (~ 0.3 ; Fig. 5). The response was always tonic in FS neurons, whereas PYR neurons at high rates exhibit a phasic component in the first few hundred milliseconds (Fig. 6). Finally, as opposed to PYR neurons, initial adaptation and early facilitation were absent in FS cells.

TABLE 3. Summary of the models of the temporal properties of the response of FS and PYR neurons

	FS	PYR
τ fA, ms	$G(180,40)$	$G(48,25)$
τ F, ms	—	$(0.198x + 400) \pm 0.53$
τ sA, s	$0.6G(2.1,0.9) + 0.4G(12.1,6.2)$	$(7.685e^{-0.000408x}) \pm 0.58$
δm_I , pA	—	$-0.107385x - 95.6 \pm 1.1$
α fA, pAs	$G(0.04,0.04)$	$G(10.6,5.5)$
$ \alpha $ F, pAs	—	$G(7.1,4.4)$
α sA, pAs	$G(0.57,0.27)$	$(0.00438x + 0.145) \pm 1$

The results are reported as (combinations of) Gaussian distributions, $G(\text{mean},SD)$, for input-independent parameters, and as “models” for input-dependent parameters, i.e., for parameters significantly correlated with input current (see the text). The models were exponential curves, $Y(x) = ae^{-bx}$, for decreasing variables, or straight lines, $Y(x) = ax + b$, for increasing variables, where a, b are constants and $x = m_I - I_{rh}$ (pA), with ranges: 0–200 pA (FS, L5), 0–250 pA (FS, L2/3), and 0–3 nA (PYR). The model for each input-dependent parameter is reported as model \pm CV, where CV is the ratio SD/mean for that parameter, and gives a measure of its variability across different recordings and different neurons. δm_I , is the corrective term that accounts for strong initial adaptation in PYRneurons.

Adaptation in the presence of input fluctuations

In FS interneurons, the amount of input fluctuations was found to correlate with the type of adaptation taking place: faster adaptation disappears in the presence of large fluctuations, whereas slower adaptation remains just as strong (see *Effect of input fluctuations on adaptation*). In pyramidal neurons, we found no evidence that input fluctuations would disrupt any of the adaptation/facilitation processes. This is consistent with the presence of slow adaptation found in vivo by Descalzo et al. (2005). Tang et al. (1997) reported that in the presence of input fluctuations, adaptation was much reduced in rat visual cortical neurons. This statement pertains to fast adaptation only, as these authors did not study prolonged firing patterns. Their analysis was based on the comparison between the spike count in the first and second halves of the total stimulus duration (900 ms). With a slightly different analysis based on cumulative ISIs durations (see RESULTS), we found

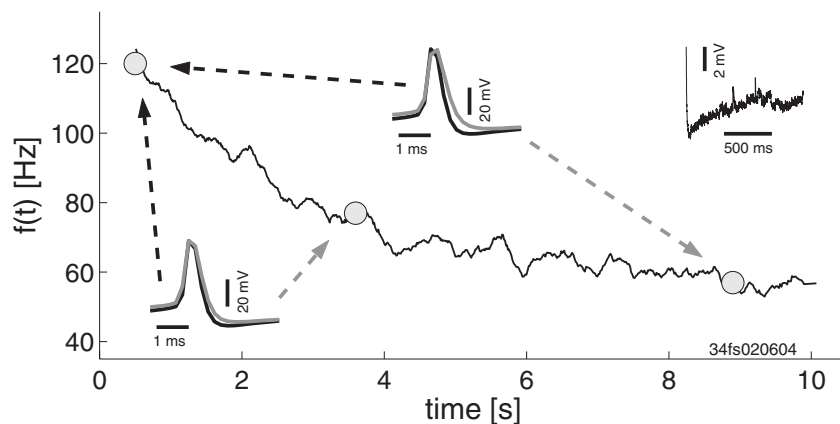


FIG. 10. Putative mechanisms underlying slow adaptation in FS neurons. The instantaneous firing rate of a L2/3 FS cell in response to a long-lasting stimulus (10 s) is shown ($m_I = 300$ pA, $s_I = 0$). *Left and middle insets*: difference in spike shape (DSS) between 0.5 (black) and 3.6 s (gray; *left inset*), and between 0.5 and 8.8 s (*middle inset*); average spike shape over 20 consecutive spikes, starting at the mentioned times. The corresponding firing rates are marked with a circle. A DSS could be the signature of slow inactivation of ion channels responsible for action potential generation (see the text). *Right inset*: presence of an AHP current after the removal of the stimulus.

that the fraction of spike trains that were categorized as fast adapting was the same in the presence and in the absence of input fluctuations. This indicates that fluctuating inputs do not disrupt adaptation but does not rule out its reduction for a given range of input parameters, as claimed by Tang et al. (1997). Factors like a different range of input currents, the different preparation (visual versus somatosensory neurons), and slightly different pipette solutions should also be taken into account while comparing the two studies.

Putative mechanisms of adaptation in FS neurons

Slow adaptation in FS neurons was found to be associated to a slow duration afterhyperpolarization (sAHP) current in ferret visual cortex (Descalzo et al. 2005). We also observed an sAHP current in FS neurons and found indirect evidence for a slow inactivation of ion currents responsible for action potential generation (Fleiderovich et al. 1996; Schwindt et al. 1997) (see Fig. 10).

The fact that occasionally sAHP was not visible at the end of stimulation (for instance, it is not visible in Figs. 1 and 2, C) does not necessarily rule out its presence. For example, no sAHP is visible in Fig. 1C (MODEL) even though it was present in the model. Typically, in such a case a more prolonged stimulation is sufficient to reveal the presence of sAHP as well as a difference in spike shape (DSS) between the beginning and the end of stimulation (see e.g., Fig. 10, *left vs. middle inset*). A DSS means that the average spike shapes, at the end and at the beginning of the spike train, are visibly different (usually wider toward the end). Such a difference could be the signature of slow inactivation of Na^+ channels (or other ionic channels responsible for action potential generation), and was consistently found in those PYR neurons which would eventually stop firing after prolonged stimulation (see Rauch et al. 2003; their Fig. 3B). When the same neurons were stimulated for longer time intervals (e.g., 10 s instead of 4), both an sAHP and a DSS were found in almost all of the recordings above a critical frequency (~ 50 Hz), as shown in Fig. 10 (note how only a negligible DSS is to be seen after 4 s). This strongly points to the presence of the postulated adapting processes even when they are not visible in recordings of shorter duration.

Putative mechanisms of early facilitation in PYR neurons

Firing rate facilitation in neocortical neurons is not usually reported in the literature. However, we found the phenomenon

to be present in response to almost all input currents and with three different pipette solutions (Rauch et al. 2003). Phenomena that resemble early facilitation have been described in noncortical neurons, where they lead to afterdepolarizations and plateau potentials, often involved in the production and control of burst discharge conditional on backpropagation of dendritic spikes (e.g., Noonan et al. 2003 and refs. therein). Mechanisms found to underlie these types of facilitatory activity are a slow activation of calcium currents (Rekling and Feldman 1997; Svirskis and Hounsgaard 1997) and a persistent sodium current (Doiron et al. 2003). Although with seemingly different functional purposes, it is possible that the same mechanisms underlie early facilitation in regular spiking neocortical neurons.

Mechanistic description

Despite the differences, PYR neurons [from acute slices (Rauch et al. 2003) and dissociated cultured networks (Giugliano et al. 2004)] and FS neurons could be described by a simple IF model with adaptation/facilitation components that is easy to simulate and amenable to theoretical analysis (La Camera et al. 2004a). Such an approach represents a notable difference with the approach usually taken in the literature, where the time course of adaptation is characterized by the firing rate reduction over time, and typically in response to DC stimulation only. In our study, we did not fit directly the firing rate over time but fitted a model endowed with rate-dependent modifications of the input current, which in turn are responsible for the observed adaptation/facilitation of the firing rate. In general, the time constants defined in these two different ways need not be the same, although are probably correlated. This might also explain the differences with other studies; in particular, why other authors have found only one time constant (e.g., Descalzo et al. 2005; Sanchez-Vives et al. 2000).

In-vivo-like stimulation

The stimulation used was meant to emulate the heavy synaptic bombardment experienced by cortical neurons in the intact brain. Synaptic currents in the cortex have a finite correlation length, ranging from a few ms (e.g., AMPA- and GABA_A -receptor mediated) to several hundreds of ms (e.g., NMDA and GABA_B receptor mediated). However, because temporal correlations in the input are partially reflected in the output spike train (La Camera et al. 2002; Salinas and Se-

jnowski 2002; Svirskis and Rinzel 2000), we chose stimuli with virtually no temporal correlation, i.e., resembling white noise. This was necessary not to interfere with the temporal properties of the response. Moreover, modeling studies (Renart et al. 2003) have shown that the white-noise driven response can be used to predict the dynamics of a network of neurons with AMPA-, GABA_A-, and NMDA-like receptor mediated current, also when adaptation is included (La Camera et al. 2004a). The issue of whether things would change when conductance injection is used in experiment (see e.g., Robinson and Kawai 1993; Sharp et al. 1993), has been addressed recently in a series of works. In one direction, the importance of conductance fluctuations (as opposed to current fluctuations) has been minimized (Richardson 2004); in another direction, it has been shown that a network of conductance-driven neurons can be mapped onto a network of current-driven neurons which have the same response functions (La Camera et al. 2004b; Rauch et al. 2003).

Modified LIF neuron

Although lacking biophysical detail, the modified LIF neuron employed in this study proved very effective at reproducing the firing behavior of cortical neurons, confirming the results of previous studies (e.g., Giugliano et al. 2004; Holt et al. 1996; Jolivet et al. 2006; Rauch et al. 2003) and extending those results to the temporal domain of the firing rate response (see also Sakai et al. 1999; Jolivet et al. 2006). According to our findings, the modified LIF neuron is the simplest model neuron that can capture the firing behavior of cortical neurons in response to stationary, in-vivo-like stimuli. In our context, this model represents an appropriate trade-off: a simpler model, for example a LIF without adaptation, might not even capture the stationary response function (Rauch et al. 2003); whereas a more biophysically grounded model would be too complex to be used in theoretical studies (in fact, the fitting procedure of this study would have not been possible because of the lack of analytical results like e.g., *Eq. 4*). Related models of spiking neurons of similar complexity and power as the modified LIF neuron could also be used, as long as the response function is known (La Camera et al. 2004a). We emphasize that even though cortical input is temporally correlated (e.g., Destexhe and Paré 1999, 2000; Destexhe et al. 2001; Paré et al. 1998; Salinas and Sejnowski 2002; Stern et al. 1998; Svirskis and Rinzel 2000), closed formulae for the white noise-driven response function like *Eq. 4* should not be dismissed: it has been shown that the (adapting) firing rate in response to “colored” inputs can be obtained by modeling the input current as temporally correlated (for example, as an Ornstein-Uhlenbeck process), but using the response function of the (adapted) white-noise driven LIF neuron, *Eqs. 3 and 4* (La Camera et al. 2004a; Renart et al. 2003).

The use of the neuron effective parameters is a way to compensate for the lack of biophysical detail in the IF model. Given the absence of correlations between “effective” and “directly estimated” parameters, our results indicate that the former should be preferred in theoretical studies if the aim is to reproduce the behavior of cortical neurons embedded in an in-vivo-like environment. For similar quantitative reductions of cortical firing patterns, see e.g., Jolivet et al. (2004).

Computational consequences of multiple time scales

The temporal processes and the wide distributions of their time constants found in this work may be linked to an already rich repertoire of experimental findings, among which the stimulus-specific adaptation of auditory cortex neurons that spans several temporal decades (Ulanovsky et al. 2004) or the long-range correlations in firing rate of, e.g., cat auditory nerves and LGN (Lowen and Teich 1996; Lowen et al. 2001). In LGN, the correlation length can be hundreds of seconds, also in the absence of sensory stimulation (Lowen et al. 2001). Those long-range correlations are only slowly reduced by averaging the spike train over progressively longer time windows, a signature of fractal behavior, i.e., due to one or more dynamical processes showing scale-free statistics. Scale-free adaptation has also been found in both vertebrate and invertebrate peripheral sensory systems (Thorson and Biederman-Thorson 1974; Xu et al. 1996), where it has been argued to be the consequence of a multitude of (adapting) exponential processes the time constants of which span several decades (Thorson and Biederman-Thorson 1974).

The results of this study encompass a broad range of time scales (spanning milliseconds to tens of seconds) but cannot provide direct evidence for scale-free adaptation, which would require stimulations of extremely long duration (ideally, infinite). Stimulus duration was limited by the protocol (the maximal stimulus duration was 10 s) in an effort to provide a quantitative description without overfitting the data, as explained in *METHODS*. Different experiments might expose other mechanisms which work on longer time scales, e.g., hundreds of seconds (Lowen et al. 2001; Ulanovsky et al. 2004). However, even a few multiple time scales—and sometimes just one of the single processes characterized here—can have a wide range of computational consequences, some of which are mentioned in the following text.

Neural codes that adapt on multiple time scales optimize the information that the neural response carry about both the rapid and the slow modifications of the external environment (Brenner et al. 2000; Fairhall et al. 2001), possibly allowing an efficient representation of real world environments that change on a variety of different time scales. Multiple time scales can be also used to extract the envelope of a signal, to distinguish between common and rare stimuli, and to link stimuli separated in time by several seconds (Drew and Abbott 2006). Reutimann et al. (2004) exploited the slow adaptation of inhibitory neurons to build a model of climbing persistent activity in primate infero-temporal cortex, proposed as the neural mechanism to encode the time interval between two relevant events. Cellular facilitation in PYR neurons, alongside with synaptic mechanisms with comparable kinetics (Wang 1999), might help sustain persistent activity, a network state that might mediate working memory (Amit 1995; Amit and Brunel 1997; Wang 2001). The same facilitation process might have a role in shaping cortical UP states (Sanchez-Vives and McCormick 2000) and “cortical flashes” (where only a small number of neurons are coactive in the UP state) (Cossart et al. 2003), even though these states are believed to be recurrent-network properties, made possible by both glutamatergic and GABAergic synaptic transmission (Cossart et al. 2003).

At least some of these computational consequences rely on the possibility that single neurons or populations are able to

respond at all time scales. Although our phenomenological description allowed us to cluster all the temporal processes in only four groups with distinct characteristics, the distributions of the model parameters are broad and have considerable overlap after the units are rescaled for comparison (Fig. 8). Hence even if the neurons studied in this work could express temporal properties with only a limited number of distinct time scales, a much larger spectrum, approximating a continuum of time scales, could be found at the population level by pulling together the activity of many neurons, each occurring to be in a different adapting state.

An alternative description of our results could be given by the presence of one or just a few adaptation mechanisms that modify dynamically their inherent time constant depending on the stimulation history (Gilboa et al. 2005; Millhauser et al. 1988). At the phenomenological level, we cannot discriminate a discrete set of processes, each with a fixed time constant, from a single mechanism with a history-dependent time constant. However, whatever this mechanism might be, its effects should be compatible with our results.

Finally, gaps in the distribution of time constants, however originated, could be covered by other dynamical processes, like those of dynamic synapses, especially in light of the recent proposal (Fusi et al. 2005) that a cascade of synaptic processes can represent a multitude of time scales much in the same way as, we argued here, adaptation in single neurons.

APPENDIX

Derivation of Eq. 2

Let T be the total stimulation time and \bar{f} the mean output rate of the neuron. We will find an approximate confidence interval on f by means of a binomial model for spike emission. Let N_{sp} be the number of spikes observed in the time interval T , and assume that T can be divided in n elementary intervals where at most one spike can be observed, with probability p : then $\bar{p} = N_{sp}/n$ is the average estimated probability of having a spike in an elementary interval. When the firing activity of the neuron is stationary, p is constant and equals \bar{p} in all elementary intervals, i.e., \bar{p} is an estimate of the stationary firing rate, $f = N_{sp}/T$, and its 68% confidence interval, $p_- \leq \bar{p} \leq p_+$, gives a 68% confidence interval for f . Given the bimodal model for p, p_{\pm} are the solution of

$$\frac{|\bar{p} - p|}{\sqrt{p(1-p)/n}} = k \quad (A1)$$

i.e.

$$p_{\pm} = \frac{\bar{p}n + k^2/2 \pm k\sqrt{\bar{p}(1-\bar{p})n + k^2/4}}{n + k^2} \quad (A2)$$

where k is the number of SDs from \bar{p} . In the well-known limit of an infinite number of elementary intervals, $n \rightarrow \infty$, with $p \rightarrow 0$ and $pn = N_{sp}$, we can use the Gaussian approximation to the binomial distribution, and derive that $k = 1$ gives the wanted confidence interval of 68%

$$P\left[\frac{|\bar{p} - p|}{\sqrt{p(1-p)/n}} \leq 1\right] \approx \frac{1}{\sqrt{2\pi}} \int_{-1}^1 e^{-t^2/2} dt \approx 0.68$$

Multiplying both sides of Eq. A2 by $n + k^2$, and performing the same limit, one obtains $(n + k^2)p_{\pm} \approx np_{\pm} \rightarrow N_{sp}^{\pm}$, $n\bar{p} \rightarrow \bar{N}_{sp}$ and

$$\bar{N}_{sp}^{\pm} = \bar{N}_{sp} + (k^2/2) \pm k\sqrt{\bar{N}_{sp} + (k^2/4)}$$

hence

$$\Delta N_{sp}^{\pm} = |N_{sp}^{\pm} - \bar{N}_{sp}| = |k^2/2 \pm k\sqrt{\bar{N}_{sp} + (k^2/4)}|$$

Finally, $\Delta f_{\pm} = \Delta N_{sp}^{\pm}/T$, which for $k = 1$ gives Eq. 2.

Details of the interaction between the adaptation/facilitation processes

Since initial (f_i) and final (f_f) firing rate turned out to be strongly correlated ($\rho = 0.86$, $P < 10^{-5}$ for PYR neurons, $\rho = 0.88$, $P < 10^{-5}$ for FS neurons), we will speak loosely of correlations with output rate without further specification. In the following analysis, correlations were taken as significant at the 0.5% level to compensate for multiple comparisons, but for completeness were reported also if >0.4 .

PYR NEURONS. In PYR neurons, the processes were differentially correlated with output rate, with the τ_s and their $\alpha_{\%s}$ anti-correlated. $\alpha_{F\%}$ was anti-correlated with f_i (-0.46 , $P < 10^{-2}$): the higher the output rate, the less prominent contribution of F , and the slower because τ_F and $\alpha_{F\%}$ were anti-correlated ($\rho = -0.52$, $P < 10^{-5}$). As a result, τ_F had a positive correlation with output rate (although not significant, $\rho = 0.2$, $P = 0.07$). Similarly, fA had anti-correlated $\alpha_{\%}$ and τ ($\rho = -0.34$, $P = 0.003$): the larger one process's contribution, the faster. However, neither $\alpha_{fA,\%}$ nor τ_{fA} were correlated with output rate. Finally, $\alpha_{sA,\%}$ was positively correlated with output rate (0.57 , $P < 10^{-5}$): the higher the output rate, the larger the relative contribution of sA compared with the other processes (mainly F, because $fA_{\%}$ and output rate were not correlated). $\tau_{sA,\%}$ was significantly anti-correlated with f_i (-0.53 , $P < 10^{-5}$): at high rates, sA becomes more prominent and faster. However, $\alpha_{sA,\%}$ and τ_{sA} were not correlated ($\rho = -0.1$, $P = 0.4$).

FS NEURONS. As opposed to PYR neurons, the $\alpha_{\%s}$ were not correlated with output rate in FS interneurons. Also, $\alpha_{fA,\%}$ and its time constant were positively correlated ($\rho = 0.59$, $P = 0.02$), i.e., a larger contribution of fast adaptation had a tendency to be slower, as opposed to PYR neurons. τ_{fA} was anti-correlated with firing rate ($\rho = -0.48$, $P = 0.068$), similarly to τ_{sA} in PYR neurons (where τ_{fA} was not correlated with output rate). Hence, fA in interneurons retains some of the features of slow adaptation in PYR neurons. No pairwise correlations were found among the sA parameters, whether the time constants were considered separately ($\tau_{sA}^{(1)}$ and $\tau_{sA}^{(2)}$) or not. In summary, recordings with larger output rates had a tendency to be dominated by sA, with less (but faster) fA. Note that only 30% of the FS cells had fA, which produced a rather small sample for this particular analysis. This might explain why substantial correlations were not found significant at the 0.5% level.

Details of the dependence of adaptation/facilitation on input current

PYR NEURONS. In PYR neurons, if the correlation with $m_I - I_{th}$ was significant (i.e., $P < 0.005$), so was the correlation with m_I . The strongest dependence on input current was found for slow adaptation: α_{sA} (4.2 ± 4.3 pA, range: 0–20 pA) was correlated with $m_I - I_{th}$ ($\rho = 0.53$, $P < 10^{-5}$), and so was $\alpha_{sA,\%}$ ($\rho = 0.44$, $P < 10^{-4}$); τ_{sA} was anti-correlated with $m_I - I_{th}$ ($\rho = -0.51$, $P = 0.0001$).

Early facilitation also had a clear dependence on input current: τ_F was correlated with $m_I - I_{th}$ ($\rho = 0.35$, $P < 0.003$), whereas $\alpha_{F,\%}$ was anti-correlated with $m_I - I_{th}$ ($\rho = -0.37$, $P < 0.0006$). However, the actual value of $|\alpha_{F\%}|$ (7.1 ± 4.4 pA, range: 0–22.6 pA) was not correlated with input current ($\rho = 0.05$, $P = 0.64$). In other words, the relative contribution of F decreases with input current (due to an increase in sA), but its absolute value fluctuates around a constant value throughout the input range. Hence, $|\alpha_{F\%}|$ was modeled as a Gaussian-distributed variable independent of input current.

Finally, fast adaptation was not correlated with input current. The distributions of the parameters were Gaussian-like (see Fig. 8), with $\alpha_{fA} = 10.6 \pm 5.5$ pA (range: 0–20.7 pA). Note that the algebraic sum

of the three α s is 7.7 ± 6.8 pA, consistent with the results of Table 1 (PYR, L5).

FS NEURONS. In FS interneurons, none of the parameters were correlated with either m_I or with $m_I - I_{th}$. As a consequence, as a “model” of these parameters we report the Gaussian distribution that best fit the data (refer to Fig. 8 for the following).

α_{sA} had a multi-peak distribution, with the largest peak around ~ 0.5 pAs. Its secondary peaks were neglected in the model. The two distributions $\alpha_{sA}\{\tau = \tau_{sA}^{(1)}\}$ and $\alpha_{sA}\{\tau = \tau_{sA}^{(2)}\}$ overlap (not shown), and no special relationship was there between α_{sA} and either $\tau_{sA}^{(1)}$ or $\tau_{sA}^{(2)}$, hence we pulled all α_{sA} values together.

α_{fA} (range: 0–0.32 pA) had approximately a Gaussian distribution centered at high values by a tail accounting for $<10\%$ of the total count. Apart from this tail, the distribution was very narrow around the main peak, ~ 0.04 , so that it could be almost described as a delta function centered in 0.04. We chose to give little weight to the tail and approximate the original distribution with a Gaussian with mean 0.04 and SD 0.04. The bimodal distribution of τ_{sA} was well approximated by the sum of two Gaussian distributions with 60 and 40% weight, respectively, see Table 3. τ_{fA} had a narrow, Gaussian-like distribution around a major central peak, and its secondary peaks were neglected.

ACKNOWLEDGMENTS

We thank Drs. Larry Abbott and Patrick Drew for inspiring discussions and a careful reading of the manuscript.

Present addresses: A. Rauch, Max Planck Institute for Biological Cybernetics, Tübingen, Germany; D. Thurbon, The Scripps Research Institute, La Jolla, CA; and S. Fusi, Center for Theoretical Neuroscience, Columbia University School of Medicine, 1051 Riverside Dr., New York, NY 10032 and Institute of Neuroinformatics, ETH/University of Zürich, Zürich, Switzerland.

GRANTS

This work was supported by Swiss National Science Foundation Grants 31–61335.00 and 3152–065234.01.

REFERENCES

- Amit D.** The hebbian paradigm reintegrated: local reverberations as internal representations. *Behav Brain Sci* 18: 617–657, 1995.
- Amit D and Brunel N.** Model of global spontaneous activity and local structured (learned) delay activity during delay. *Cereb Cortex* 7: 237–252, 1997.
- Bowman AW and Azzalini A.** *Applied Smoothing Techniques for Data Analysis*. Oxford, UK: Oxford Univ. Press, 1997.
- Brenner N, Bialek W, and de Ruyter van Steveninck R.** Adaptive rescaling maximizes information transmission. *Neuron* 26: 695–702, 2000.
- Cossart R, Aronov D, and Yuste R.** Attractor dynamics of network UP states in the neocortex. *Nature* 423: 283–288, 2003.
- Cox DR and Miller HD.** *The Theory of Stochastic Processes*. New York: Chapman and Hall, 1965.
- Descalzo V, Nowak L, Brumberg J, McCormick D, and Sanchez-Vives M.** Slow adaptation in fast spiking neurons in visual cortex. *J Neurophysiol* 93: 1111–1118, 2005.
- Destexhe A and Paré D.** Impact of network activity on the integrative properties of neocortical pyramidal neurons in vivo. *J Neurophysiol* 81: 1531–1547, 1999.
- Destexhe A and Paré D.** A combined computational and intracellular study of correlated synaptic bombardment in neocortical pyramidal neurons in vivo. *Neurocomputing* 32: 113–119, 2000.
- Destexhe A, Rudolph M, Fellous JM, and Sejnowski TJ.** Fluctuating dynamic conductances recreate in vivo like activity in neocortical neurons. *Neuroscience* 107: 13–24, 2001.
- Doiron B, Noonan L, Lemon N, and Turner R.** Persistent Na^+ current modifies burst discharge by regulating conditional backpropagation of dendritic spikes. *J Neurophysiol* 89: 324–337, 2003.
- Drew PJ and Abbott LF.** Models and properties of power-law adaptation in neural systems. *J Neurophysiol* doi:10.1152/jn.00134.2006, 2006.
- Ermentrout B.** Linearization of f-I curves by adaptation. *Neural Comput* 10: 1721–1729, 1998.
- Fairhall A, Lewen G, Bialek W, and de Ruyter van Steveninck R.** Efficiency and ambiguity in an adaptive neural code. *Nature* 412: 787–792, 2001.
- Fleiderovich I, Friedman A, and Gutnick M.** Slow inactivation of Na^+ current and slow cumulative spike adaptation in mouse and guinea-pig neocortical neurons in slices. *J Physiol* 493: 83–97, 1996.
- Fuhrmann G, Markram H, and Tsodyks M.** Spike frequency adaptation and neocortical rhythms. *J Neurophysiol* 88: 761–770, 2002.
- Fusi S, Drew PJ, and Abbott LF.** Cascade models of synaptically stored models. *Neuron* 45: 1–14, 2005.
- Gabbiani F and Koch C.** Principles of spike train analysis. In: *Methods in Neuronal Modeling: From Synapses to Networks* (2nd ed.), edited by Koch C and Segev I. Cambridge, MA: MIT Press, 1998, p. 313–360.
- Gershon E, Wiener M, Latham P, and Richmond B.** Coding strategies in monkey V1 and inferior temporal cortices. *J Neurophysiol* 79: 1135–1144, 1998.
- Gilboa G, Chen R, and Brenner N.** History-dependent multiple-time-scale dynamics in a single-neuron model. *J Neurosci* 25: 6479–6489, 2005.
- Giugliano M, Darbon P, Arsiero M, Lüscher HR, and J Streit J.** Single-neuron discharge properties and network activity in dissociated cultures of neocortex. *J Neurophysiol* 92: 977–996, 2004.
- Gur M, Beylin A, and Snodderly D.** Response variability of neurons in primary visual cortex (V1) of alert monkeys. *J Neurosci* 17: 2914–2920, 1997.
- Haider B, Duque A, Hasenstaub AR, and McCormick DA.** Neocortical network activity in vivo is generated through a dynamic balance of excitation and inhibition. *J Neurosci* 26: 4535–4545, 2006.
- Holt G, Softky W, Koch C, and Douglas R.** Comparison of discharge variability in vitro and in vivo in cat cortex neurons. *J Neurophysiol* 75: 1806–1814, 1996.
- Hsu SM, Raine L, and Fanger H.** The use of avidin-biotin-peroxidase (ABC) in immunoperoxidase techniques: a comparison between ABC and unlabelled antibody (peroxidase) procedures. *J Histochem Cytochem* 29: 577–590, 1981.
- Iansek R and Redman SJ.** An analysis of the cable properties of spinal motoneurons using a brief intracellular current pulse. *J Physiol* 234: 613–636, 1973.
- Jolivet R, Lewis T, and Gerstner W.** Generalized integrate-and-fire models of neuronal activity approximate spike trains of a detailed model to a high degree of accuracy. *J Neurophysiol* 92: 959–976, 2004.
- Jolivet R, Rauch A, Lüscher HR, and Gerstner W.** Predicting spike timing of neocortical pyramidal neurons by simple threshold models. *J Comput Neurosci* DOI: 10.1007/s10827-006-7074-5, 2006.
- La Camera G, Fusi S, Senn W, Rauch A, and Lüscher HR.** When NMDA receptor conductances increase inter-spike interval variability. In: *Proceedings of ICANN 2002, LNCS 2415*, edited by Dorransoro JR. New York: Springer-Verlag, 2002, p. 235–240.
- La Camera G, Rauch A, Senn W, Lüscher HR, and Fusi S.** Minimal models of adapted neuronal response to in-vivo-like input currents. *Neural Comput* 16: 2101–2124, 2004a.
- La Camera G, Senn W, and Fusi S.** Comparison between networks of conductance- and current-driven neurons: stationary spike rates and sub-threshold depolarization. *Neurocomputing* 58-60C: 253–258, 2004b.
- Lee D, Port N, Kruse W, and Georgopoulos A.** Variability and correlated noise in the discharge of neurons in motor and parietal areas of the primate cortex. *J Neurosci* 18: 1161–1170, 1998.
- Lerchner A, Ursta C, Hertz J, Ahmadi M, Ruffiot P, and Enemark S.** Response variability in balanced cortical networks. *Neural Comput* 18: 634–659, 2006.
- Liu YH and Wang XJ.** Spike-frequency adaptation of a generalized leaky integrate-and-fire model neuron. *J Comput Neurosci* 10: 25–45, 2001.
- Lowen S, Ozaki T, Kaplan E, Saleh B, and Teich M.** Fractal features of dark, maintained, and driven neural discharges in the cat visual system. *Methods* 24: 377–394, 2001.
- Lowen S and Teich M.** The periodogram and Allan variance reveal fractal exponents greater than unity in auditory-nerve spike trains. *J Acoust Soc Am* 99: 3585–3591, 1996.
- McCormick DA, Connors BW, Lighthall JW, and Prince D.** Comparative electrophysiology of pyramidal and sparsely stellate neurons of the neocortex. *J Neurophysiol* 54: 782–806, 1985.
- Millhauser GL, Salpeter EE, and Oswald RE.** Diffusion models of ion-channel gating and the origin of power-law distributions from single-channel recording. *Proc Natl Acad Sci USA* 85: 1503–1507, 1988.

- Noonan L, Doiron B, Laing C, Longtin A, and Turner R. A dynamic dendritic refractory period regulates burst discharge in the electrosensory lobe of weakly electric fish. *J Neurosci* 23: 1524–1534, 2003.
- Paré D, Shink E, Gaudreau H, Destexhe A, and Lang E. Impact of spontaneous synaptic activity on the resting properties of cat neocortical pyramidal neurons in vivo. *J Neurophysiol* 11: 1450–1460, 1998.
- Powers R, Sawczuk A, Musick J, and Binder M. Multiple mechanisms of spike-frequency adaptation in motoneurons. *J Physiol* 93: 101–114, 1999.
- Press W, Teukolsky S, Vetterling W, and Flannery B. *Numerical Recipes in C: The Art of Scientific Computing*. Cambridge, UK: Cambridge Univ. Press, 1992.
- Rauch A, La Camera G, Lüscher HR, Senn W, and Fusi S. Neocortical cells respond as integrate-and-fire neurons to in-vivo-like input currents. *J Neurophysiol* 90: 1598–1612, 2003.
- Rekling J and Feldman J. Calcium-dependent plateau potentials in rostral ambiguous neurons in the newborn mouse brain stem in vitro. *J Neurophysiol* 78: 2483–2492, 1997.
- Renart A, Brunel N, and Wang XJ. Mean-field theory of recurrent cortical networks: from irregularly spiking neurons to working memory. In: *Computational Neuroscience: A Comprehensive Approach*, edited by Feng J. Boca Raton, FL: CRC, 2003, p. 431–490.
- Reutimann J, Yakovlev V, Fusi S, and Senn W. Climbing neuronal activity as an event-based cortical representation of time. *J Neurosci* 24: 3295–3303, 2004.
- Richardson MJE. The effects of synaptic conductance on the voltage distribution and firing rate of spiking neurons. *Phys Rev E* 69: 051918, 2004.
- Robinson H and Kawai N. Injection of digitally synthesized synaptic conductance transients to measure the integrative properties of neurons. *J Neurosci Methods* 49: 157–165, 1993.
- Sakai Y, Funahashi S, and Shinomoto S. Temporally correlated inputs to leaky integrate-and-fire models can reproduce spiking statistics of cortical neurons. *Neural Netw* 12: 1181–1190, 1999.
- Salinas E and Sejnowski TJ. Integrate-and-fire neurons driven by correlated stochastic input. *Neural Comput* 14: 2111–2155, 2002.
- Sanchez-Vives MV and McCormick DA. Cellular and network mechanisms of rhythmic recurrent activity in neocortex. *Nat Neurosci* 3: 1027–1034, 2000.
- Sanchez-Vives M, Nowak L, and McCormick D. Cellular mechanisms of long-lasting adaptation in visual cortical neurons in vitro. *J Neurosci* 20: 4286–4299, 2000.
- Sawczuk A, Powers R, and Binder M. Contribution of outward currents to spike frequency adaptation in hypoglossal motoneurons of the rat. *J Physiol* 78: 2246–2253, 1997.
- Schwindt P, O'Brien J, and Crill W. Quantitative analysis of firing properties of pyramidal neurons from layer 5 of rat sensorimotor cortex. *J Neurophysiol* 77: 2484–2498, 1997.
- Schwindt P, Spain W, and Crill W. Long-lasting reduction of excitability by a sodium-dependent potassium current in cat neocortical neurons. *J Neurophysiol* 61: 233–244, 1989.
- Shadlen M and Newsome W. Noise, neural codes and cortical organization. *Curr Opin Neurobiol* 4: 569–579, 1994.
- Shadlen M and Newsome W. The variable discharge of cortical neurons: implications for connectivity, computation and information coding. *J Neurosci* 18: 3870–3896, 1998.
- Sharp AA, O'Neil MB, Abbott LF, and Marder E. Dynamic clamp - computer generated conductances in real neurons. *J Neurophysiol* 69: 992–995, 1993.
- Shinomoto S, Shima K, and Tanji J. Differences in spiking patterns among cortical neurons. *Neural Comput* 15: 2823–2842, 2003.
- Shinomoto S, Miyazaki Y, Tamura H, and Fujita I. Regional and laminar differences in in vivo firing patterns of primate cortical neurons. *J Neurophysiol* 94: 567–575, 2005.
- Shu Y, Hasenstaub A, and McCormick DA. Turning on and off recurrent balanced cortical activity. *Nature* 423: 288–293, 2003.
- Spain W, Schwindt P, and Crill W. Two transient potassium currents in layer V pyramidal neurones from cat sensorimotor cortex. *J Physiol* 434: 591–607, 1991.
- Stern EA, Jaeger D, and Wilson CJ. Membrane potential synchrony of simultaneously recorded striatal spiny neurons in vivo. *Nature* 394: 475–478, 1998.
- Svirskis G and Hounsgaard J. Depolarization-induced facilitation of a plateau-generating current in ventral horn neurons in the turtle spinal cord. *J Neurophysiol* 78: 1740–1742, 1997.
- Svirskis G and Rinzel J. Influence of temporal correlation of synaptic input on the rate and variability of firing in neurons. *Biophys J* 5: 629–637, 2000.
- Tang A, Bartels M, and Sejnowski T. Effects of cholinergic modulation on responses of neocortical neurons to fluctuating input. *Cereb Cortex* 7: 502–509, 1997.
- Thorson J and Biederman-Thorson M. Distributed relaxation processes in sensory adaptation. *Science* 183: 161–172, 1974.
- Ulanovsky N, Las L, Farkas D, and Nelken I. Multiple time scales of adaptation in auditory cortex neurons. *J Neurosci* 24: 10440–10453, 2004.
- van Vreeswijk C and Sompolinsky H. Chaos in neuronal networks with balanced excitatory and inhibitory activity. *Science* 274: 1724–1726, 1996.
- Victor J. Spike train metrics. *Curr Opin Neurobiol* 15: 585–592, 2005.
- Wang XJ. Synaptic basis of cortical persistent activity: the importance of NMDA receptors to working memory. *J Neurosci* 19: 9587–9603, 1999.
- Wang XJ. Synaptic reverberation underlying mnemonic persistent activity. *Trends Neurosci* 24: 455–463, 2001.
- Wiener MC, Oram MW, Liu Z, and Richmond BJ. Consistency of encoding in monkey visual cortex. *J Neurosci* 21: 8210–8221, 2001.
- Xu Z, Payne J, and Nelson M. Logarithmic time course of sensory adaptation in electrosensory afferent nerve fibers in a weakly electric fish. *J Neurophysiol* 47: 2020–2032, 1996.